Meltwater and ice rafting in the southern Norwegian Sea between 20 and 40 calendar kyr B.P.: Implications for Fennoscandian Heinrich events

W. A. H. Lekens,[1] H. P. Sejrup,[1] H. Haflidason,[1] J. Knies,[2] and T. Richter[3]

Received 22 September 2005; revised 6 March 2006; accepted 27 March 2006; published 9 September 2006.

[1] The timing of meltwater release in the southern Norwegian Sea in relation to millennial-scale climate variability is studied from core MD99-2283 based on down-core analysis of stable oxygen and carbon isotopes, calcium carbonate and ice-rafted debris (IRD). Between 20 and 40 calendar (cal) kyr B.P., strong Dansgaard-Oeschger cyclicity is expressed in increased carbonate content and reduced total organic carbon during warm interstadials and IRD marking the end of cold stadials. The planktonic $\delta^{18}O$ record of core MD99-2283 compared to available isotopic records in the region confirms the existence of multisourced, synchronized meltwater anomalies during Heinrich (H) events 2 to 4. It was found that the sudden release of meltwater occurs near major ice streams and that no significant increase in IRD was associated with the peaks of the meltwater events in the southern Norwegian Sea, suggesting meltwater discharges from ice-dammed lakes. Significant meltwater events not related to the H events were also observed between 33 and 35 cal kyr B.P., indicating that the release of meltwater is not necessarily connected with major cooling and enhanced IRD delivery. The simultaneous release of fresh water during H events in the Nordic Seas, through icebergs and ice-dammed lakes, is thought to be the result of sea level increase. The meltwater input to the Nordic Seas provides a significant additional contribution to global sea level rise associated with H3 and H4.

Citation: Lekens, W. A. H., H. P. Sejrup, H. Haflidason, J. Knies, and T. Richter (2006), Meltwater and ice rafting in the southern Norwegian Sea between 20 and 40 calendar kyr B.P.: Implications for Fennoscandian Heinrich events, *Paleoceanography*, *21*, PA3013, doi:10.1029/2005PA001228.

1. Introduction

[2] Ice cores, marine and terrestrial records of the last glacial period are characterized by strong periodic oscillations in temperature called Dansgaard-Oeschger (D-O) cycles. These cycles have a periodicity of around 1470 years [*Grootes and Stuiver*, 1997] and are coupled with changes in air temperature of $10° \pm 4°C$ in Greenland [*Johnsen et al.*, 2001; *Grachev and Severinghaus*, 2005] and 2° to 4°C in the sea surface temperatures of the North Atlantic [*Sachs and Lehman*, 1999; *van Kreveld et al.*, 2000]. Progressively colder D-O cycles are grouped in "Bond" cycles, with the end of each cycle punctuated by massive ice calving events in the North Atlantic known as "Heinrich" events [*Bond et al.*, 1993]. Millennial-scale variability associated with the D-O events has been reported globally [*Voelker*, 2002], throughout interglacials and during the Pleistocene [*Oppo et al.*, 1998; *Draut et al.*, 2003]. Different forcing mechanisms for the D-O and Heinrich events (H) have been suggested, ranging from independent ice sheet dynamics [*Alley and MacAyeal*, 1994], sea ice variability [*Kaspi et al.*, 2004], extraterrestrial forcing [*Berger et al.*, 2002; *Berger and von Rad*, 2002; *Rahmstorf*, 2003] and disruptions in the thermohaline circulation [e.g., *Broecker et al.*, 1990]. Coupling and decoupling of different oscillations provides a way of conciliating the different forcing mechanisms [*Schulz*, 2002; *Schulz et al.*, 2004] and modeling indicates that the basic structure and timescale of the D-O variability is due to internal, self sustained oscillations in the ocean-atmosphere system [*Olsen et al.*, 2005]. This is supported by the observed increased amplitude and variability of the D-O cycles associated with sea levels between 30 and 50 m below the present [*McManus et al.*, 1999; *Schulz et al.*, 1999; *Chappell*, 2002].

[3] Modeling demonstrates that the ocean thermohaline circulation is sensitive to freshwater input in the Northern Hemisphere [*Ganopolski and Rahmstorf*, 2001; *Claussen et al.*, 2003; *Knutti et al.*, 2004; *Roche et al.*, 2004] and freshwater input is thought to lead to observed disruptions in the thermohaline circulations during Heinrich events [*Broecker et al.*, 1990, 1992; *Ganopolski and Rahmstorf*, 2001]. Large freshwater inputs have been associated with both the release of large numbers of icebergs to the ocean [*Cortijo et al.*, 1997; *Kanfoush et al.*, 2000] and/or the catastrophic draining of ice-dammed lakes and subglacial meltwater [e.g., *Mangerud et al.*, 2004]. The release of large numbers of icebergs has been ascribed to binge-purge oscillations of ice streams [*Alley and MacAyeal*, 1994], ice shelf collapse [*Scambos et al.*, 2000; *Hulbe et al.*, 2004] and increased ice stream calving due to warming [*Dowdeswell and Elverhøi*, 2002] and/or sea level rise

[1]Department of Earth Science, University of Bergen, Bergen, Norway.
[2]Geological Survey of Norway, Trondheim, Norway.
[3]Royal Netherlands Institute for Sea Research, Den Hoorn (Texel), Netherlands.

0883-8305/06/2005PA001228

[*Hughes*, 2002]. Remains of ice-dammed lakes, on the other hand, have been observed in association with the Laurentide ice sheet [*Teller*, 1995; *LaRocque et al.*, 2003] and the Eurasian ice sheets [*Mangerud et al.*, 2001; *Houmark-Nielsen and Kjaer*, 2003; *Clark et al.*, 2004; *Mangerud et al.*, 2004]. In addition, sudden outburst of fresh water from such lakes is supported by a growing body of evidence [*Barber et al.*, 1999; *Geirsdottir et al.*, 2000; *Blais-Stevens et al.*, 2003; *Knies and Vogt*, 2003; *Spielhagen et al.*, 2004].

[4] On the basis of reconstructions from core MD99-2283, from the northern North Sea margin, this paper investigates the role of the Norwegian Channel Ice Stream (NCIS) and the southern Fennoscandian ice sheet in meltwater delivery to the southern Norwegian Sea. In combination with available regional data, the locations and rate of the meltwater input to the Nordic Seas can be reconstructed, providing new information on the effect of the ice sheet configuration in the regions and the impact of meltwater release on oceanic conditions.

2. Material and Methods

[5] Core MD99-2283 was taken at 62°15.67′N and 0°24.84′E during the 1999 International Marine Past Global Changes Study (IMAGES V) cruise using a Calypso giant piston corer (Figure 1) and is compared to high-resolution records in the region (Table 1). The core was raised from a water depth of 707 m, taken in a hemipelagic deposit about 2 km southwest of the edge of the North Sea Fan. The core site is positioned just north of the Faroe-Shetland Channel and monitors the inflow of North Atlantic water to the Nordic Seas. The core has a length of 27.5 m and the top 15 m will be discussed here.

2.1. Sedimentological Analysis

[6] Gamma ray density was determined on board every 2 cm using a Geotek Multi Sensor Core Logger [*Best and Gunn*, 1999]. X rays were taken of split cores and used to describe sedimentary structures and count the number of ice rafted debris (IRD) larger then 2 mm [*Grobe*, 1987]. The X-ray photographs were also used to assess bioturbation and the stretching common in piston cores [*Hall and McCave*, 2000; *Auffret et al.*, 2002; *Lekens et al.*, 2005]. Cracks in the sediment were measured visibly and using X rays. From the measurement of the cracks an estimated total stretching of 2.44 m was recorded in the whole core, with the strongest stretching in the lower 10 m. The upper 15 m discussed in this paper is stretched 52.5 cm. Owing to the low extensional stress yield of the clayey material the sediment column can be reconstructed by removing the depth gaps associated with the cracks, leading to corrected depth. All data in this paper is depth corrected. The core was subsampled every 5 cm using 10 mL syringes and the samples were dried overnight at 60°C. Moisture content and density were calculated. The samples were wet sieved on 1 mm, 150 μm, 125 μm and 63 μm sieves. The fragments > 1 mm were counted every 10 cm, of which chalk >1 mm is shown here. The fine fraction was dried and analyzed using a Sedigraph 5100. Bulk accumulation rates (AR) were calculated by multiplying the linear sedimentation rate with the dry bulk density. The AR of the fraction >150 μm was calculated by multiplying the weight percentage with the AR and divide by 100 [*Ehrmann and Thiede*, 1986].

2.2. Magnetic Properties

[7] Magnetic susceptibility (k) was determined every 0.5 cm using a Geotek Multi Sensor Core Logger with a MS2E Point sensor of the University of Bergen. Using u channels the natural remanent magnetization (NRM) of core MD99-2283 was measured with a pass-through DC SQUID cryogenic magnetometer at the University of Bremen. Stepwise in line alternating field demagnetization between 5 and 70 mT was used with 12 steps. All data within 2 cm of cracks were removed. Inclination of the NRM was accepted if a minimum of 5 demagnetization steps could be used and the α_{95} was lower then 5° (calculated using principal component analysis), as to not include any overprinted or faulty data.

2.3. Geochemical Analysis

[8] Semiquantitative analysis of major and minor element composition was performed on split cores every 2 cm by means of the CORTEX core scanner [*Jansen et al.*, 1998]. Total carbon (TC) and total organic carbon (TOC) were measured on ground bulk samples and carbonate-free sediment samples using a LECO CS 244 analyzer, according to standard procedures [e.g., *Knies et al.*, 2003]. The carbonate content (%) was calculated as $CaCO_3$ (%) = (TC − TOC) × 8.33 [e.g., *Ehrmann and Thiede*, 1986].

2.4. Stable Isotope Analysis

[9] Stable oxygen and carbon isotopes of approximately 7 specimens of the planktonic foraminifera species *Neogloboquadrina pachyderma* (sinistral) (*N. pachyderma* (s)) with secondary calcite overgrowth and a size between 150 and 300 μm, were measured at the University of Bergen using a Finnigan 251 mass spectrometer. Gas for isotope measurements was produced by reaction with orthophosphoric acid at 70°C in an automated online system with acid added to the samples in individual reaction chambers. Results are reported with respect to the VPDB (Vienna Peedee belemnite) standard through calibration against the NBS19 and CM03 standard (Carrara marble). The long-term reproducibility reported by the laboratory is ±0.04‰ for the $\delta^{13}C$ and ±0.07‰ for $\delta^{18}O$, based on replicate measurements of internal standards.

3. Results and Discussion

3.1. Age Model

[10] The age model of the upper 14 m of core MD99-2283 is primarily based on 17 radiocarbon dates and the presence of the Laschamp paleomagnetic excursion. Refinement and support was provided by correlation of the Ca data to Greenland Ice Core Project (GRIP), which is supported by independent TOC data. Fifteen samples of monospecific foraminifera of the species *N. pachyderma* (s) and two samples of mollusks were accelerator mass spectrometry (AMS) radiocarbon dated to provide the initial chronologic framework (Table 2 and Figure 2). All radiocarbon dates have been corrected using a global marine

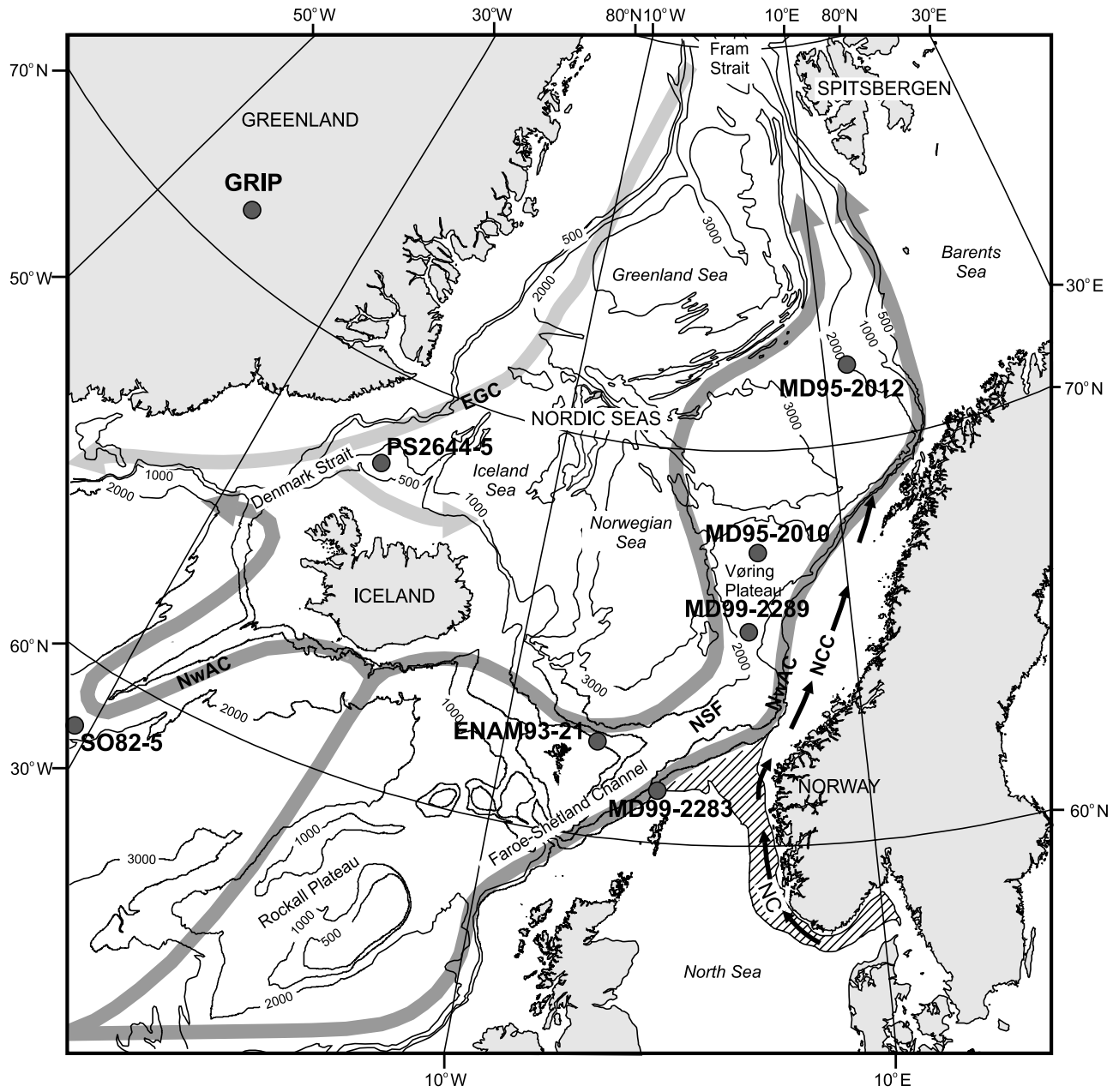

Figure 1. North Atlantic overview map showing core positions and main surface currents (shaded arrows), based on *Hopkins* [1991] and *Orvik and Niiler* [2002]. Abbreviations are EGC, Eastern Greenland Current; NC, Norwegian Channel; NCC, Norwegian Coastal Current; NwAc, Norwegian Atlantic Current; and NSF, North Sea Fan.

reservoir effect of 400 years [*Stuiver et al.*, 1998] and a ΔR value of 25 ± 81 years [*Lekens et al.*, 2005]. The radiocarbon ages were converted to calendar ages using the pristine coral $^{230}Th/^{234}U/^{238}U$ dated calibration curve and the online calibration program of *Fairbanks et al.* [2005]. A 95.4% confidence level (2σ) was calculated for the calibrated ages including the error on the ΔR (Table 2).

[11] Several studies in the region have shown that reservoir effects up to 1200 years or more have existed, especially during the last glacial/interglacial transition and potentially during Heinrich events [e.g., *Bard et al.*, 1994;

Table 1. Locations and Water Depths of Cores Used in This Study

Core	Latitude North	Longitude West	Water Depth, m
ENAM 93-21	62°44.0′	03°59.9′	1020
MD95-2010	66°41.1′	04°34.0′	1226
MD95-2011	66°58.2′	03°59.9′	1048
MD95-2012	72°02.2′	03°59.9′	2094
MD99-2283	62°15.7′	00°24.8′	707
MD99-2289	64°39.4′	04°12.6′	1262
PS2644-5	62°44.0′	03°59.9′	778
SO 82-5	62°44.0′	03°59.9′	1416

Table 2. Accelerator Mass Spectrometry Radiocarbon Dates and Tie Points Used in the Construction of the Age Model of Core MD99-2283, Upper 15 m[a]

Depth, cm	Corrected Depth, cm	Material/Proxy	Lab Number/Interpretation	^{14}C Age Uncorrected, kyr	S.D. (1σ), kyr	Calendar Age B.P., kyr	S.D. (2σ), kyr
45	44	*N. pachyderma* (s)	Poz-3945	17.08	0.07	19.69	0.44
85	84	*N. pachyderma* (s)	Poz-3946	17.36	0.07	20.07	0.39
115	114	*N. pachyderma* (s)	Poz-3947	17.75	0.08	20.46	0.3
159	158	*N. pachyderma* (s)	Poz-3948	18.19	0.08	20.94	0.56
185	184	*N. pachyderma* (s)	ETH-26404	17.68	0.14	20.39	0.44
235	227.5	*N. pachyderma* (s)	ETH-24515	18.28	0.13	21.11	0.76
355	347.5	*N. pachyderma* (s)	ETH-26405	19.74	0.15	23.07	0.81
375	367.5	δ^{18}O	H2	20.4–21.0		23.4–24.2[b]	
415	407.5	*N. pachyderma* (s)	ETH-24514	20.87	0.18	24.45	0.61
475	467.5	*N. pachyderma* (s)	Poz-7179	22.74	0.12	26.82	0.44
617	609.5	Ca/Fe, C/N	End D-O 3			27.14	0.02
635	627.5	*N. pachyderma* (s)	ETH-26406	23.67	0.22	27.79	0.65
649	641.5	Ca/Fe, C/N	Start D-O 3			27.42	0.02
683	675.5	Ca/Fe, C/N	End D-O 4			28.25	0.02
715	707.5	*N. pachyderma* (s)	ETH-24513	24.03	0.21	28.16	0.62
717	709.5	Ca/Fe, C/N	End D-O 4			28.55	0.02
764	756	Ca/Fe, C/N	Start D-O 4			29.75	0.02
775	767	*N. pachyderma* (s)	ETH-24512	26.13	0.22	30.65	0.32
810	802	δ^{18}O	H3	25.6–26.4		29.0–30.2[b]	
844	836	Ca/Fe, C/N	D-O 4a			30.34	0.02
1025	1014.5	*N. pachyderma* (s)	ETH-24511	26.82	0.25	30.96	0.31
1032	1021.5	Ca/Fe, C/N	D-O 4b			32.3	0.02
1040	1029.5	*N. pachyderma* (s)	Poz-7180	28.6	0.26	32.59	1.12
1104	1093.5	Ca/Fe, C/N	Start D-O 5			33.6	0.02
1185	1170	*N. pachyderma* (s)	Poz-3953	29.24	0.18	33.73	1.29
1235	1220	Gastropod	ETH-24516	31.52	0.28	36.37	0.92
1243	1228	Ca/Fe, C/N	End D-O 7			34.6	0.02
1259	1242.5	Ca/Fe, C/N	Start D-O 7			35.4	0.02
1297	1280	Bivalve	Poz-3954	32.44	0.23	37.35	0.96
1312	1295	Ca/Fe, C/N	End D-O 8			36.5	0.02
1407	1379.5	Ca/Fe, C/N	Start D-O 8			38.34	0.02
1415	1387.5	δ^{18}O	H4	32.4–34.2		38.4–40.0[b]	
1417	1389.5	inclination NRM	Laschamp			40.2[c]	2.00

[a]Accelerator mass spectrometry ^{14}C ages were corrected using a reservoir age of 425 ± 81 years [*Lekens et al.*, 2005] and the calibration curve of *Fairbanks et al.* [2005], version Fairbanks0605. Timing of the D-O events was determined from the δ^{18}O record of GRIP [*Johnsen et al.*, 2001]. SD is standard deviation.
[b]Source is *Sarnthein et al.* [2001].
[c]Source is *Guillou et al.* [2004].

Austin et al., 1995; *Haflidason et al.*, 1995; *Voelker et al.*, 1998; *Waelbroeck et al.*, 2001; *Björck et al.*, 2003]. While the number of radiocarbon ages in this study does not allow for a precise estimate of the reservoir effect, the resulting uncertainty can be quantified. To accommodate the uncertainties of the reservoir effect in the construction of the age model, we use the known reservoir range of modern oceans, mostly ranging between 300 and 1200 years (Figure 3) [*Bard*, 1988; *Reimer and Reimer*, 2001]. This range in addition of the radiocarbon uncertainties provides a more realistic estimate of the total uncertainty, includes most of the reported estimated reservoir effects and reflects the more certain upper limit of the radiocarbon ages.

[12] To refine the initial polynomial age model based on the radiocarbon dates, the different measured proxies were compared with records in the region. On the basis of a strong coupling of the Ca record with SST records of neighboring cores and the ice cores in Greenland, the age model can be tuned to the δ^{18}O record of GRIP, using the ss09sea age scale [*Johnsen et al.*, 2001]. The resulting correlation points fall within the previously outlined uncertainty range of the radiocarbon dates (Figure 4). Also, three strong meltwater spikes associated with the Heinrich events could be identified based on the oxygen isotope record [*Sarnthein et al.*, 1995; *Vidal et al.*, 1997; *Dokken and Jansen*, 1999; *Sarnthein et al.*, 2001] and occur stratigraphically correct in the record compared to the radiocarbon dates (Table 2). Additional support for the chronology is provided by the presence of the Laschamp paleomagnetic excursion at 1396 cm (Figure 2). Similar as to other studies the Laschamp excursion occurs prior to Heinrich event 4 in core MD99-2283 [*Kissel et al.*, 1999; *Voelker et al.*, 2000]. The Laschamp excursion is K/Ar and Ar^{39}/Ar^{40} dated to 40.4 ± 2.0 cal kyr B.P. from lava flows in France [*Guillou et al.*, 2004]. A linearly interpolated age model was constructed based on the radiocarbon dates and the different available correlation points (Figure 3). The changes in sedimentation rate and the radiocarbon dates around 30 cal kyr B.P. are considered to be less reliable because of strong changes in the ^{14}C production rate [*Hughen et al.*, 2004; *Fairbanks et al.*, 2005].

3.2. Calcium Carbonate and Organic Carbon Time Series

[13] Calcium carbonate levels lie between 9.6 and 22.5% with an average of 14.1% (Figure 4). Calcium carbonate measurements and Ca data from XRF have a regression

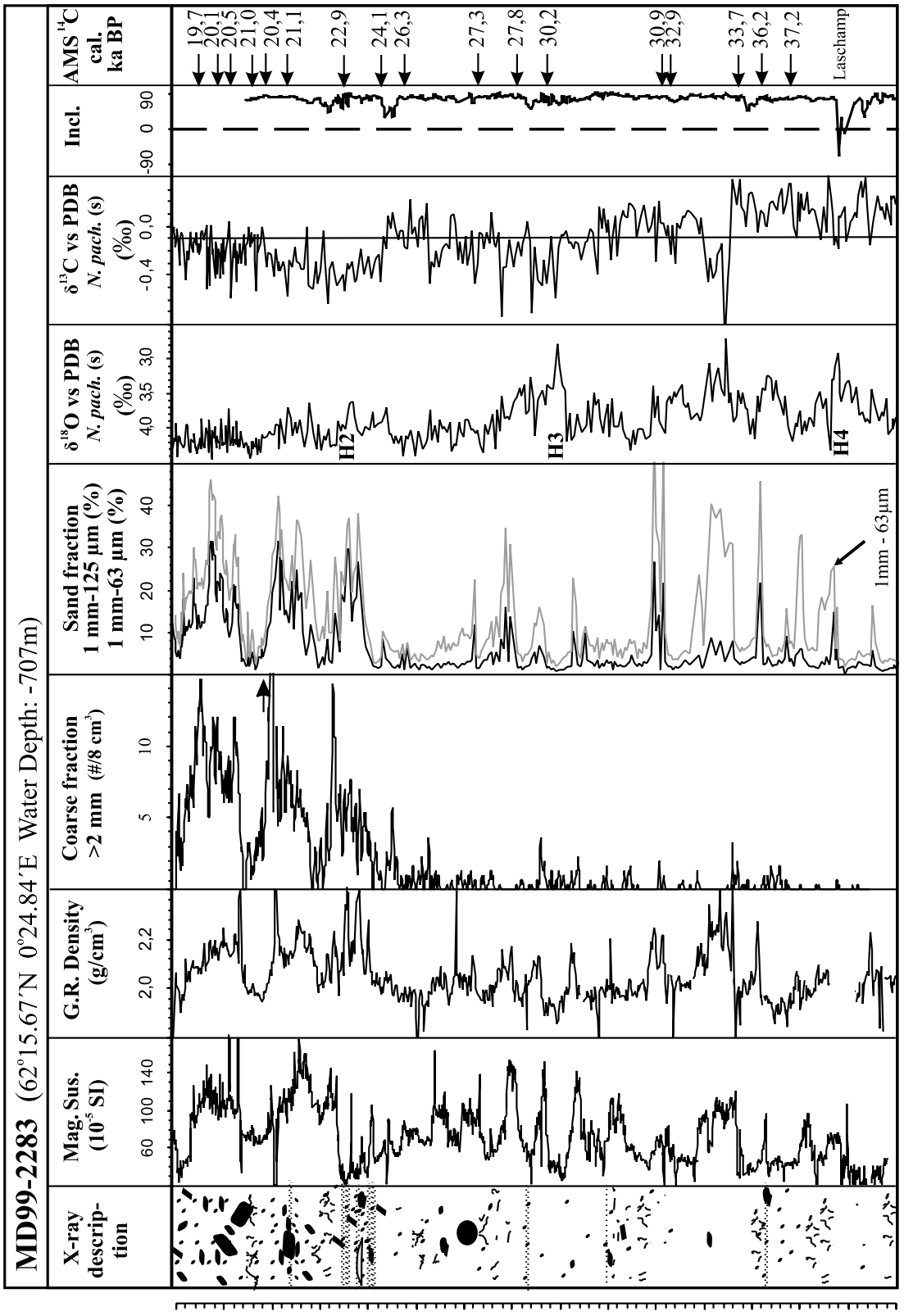

Figure 2. Sedimentological description of the upper 15 m of core MD99-2283, showing X-ray description, bioturbation and >2 mm ice-rafted detritus (IRD) counts from X rays, weight percent of the >125 µm and >63 µm fraction, oxygen and carbon isotopes measured on *N. pachyderma* (s) radiocarbon dates, and inclination data.

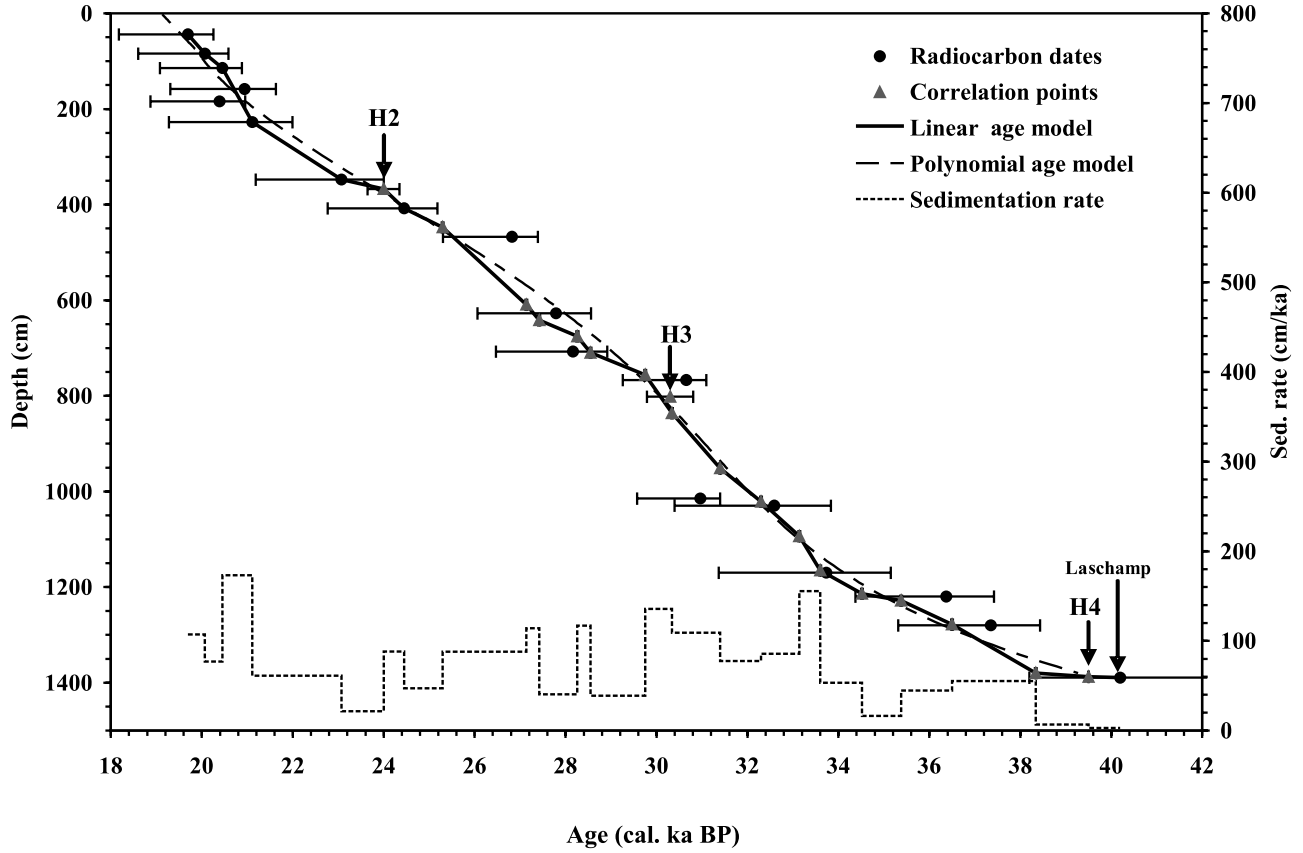

Figure 3. Age models of core MD-99-2283 together with radiocarbon accelerator mass spectrometry (AMS) dates, showing correlation points with GRIP, Heinrich events, and the Laschamp paleomagnetic excursion. Dashed line presents the best fit polynomial of the ^{14}C radiocarbon dates.

coefficient (r) of 0.59 (n = 96) and the carbonate data shows no correlation with coarse chalk, IRD or the AR (Figure 5). The correlation confirms the use of the Ca XRF data as a high-resolution semiquantitative indicator of $CaCO_3$ [*Jansen et al.*, 1998; *Richter et al.*, 2001; *Helmke et al.*, 2005]. The Ca/Fe ratio displays a much stronger signal-to-noise ratio, removes variations in water content, grain size, surface roughness and consolidation and dilution effects [see also *Jansen et al.*, 1998]. This leads to an increased correlation coefficient with the calcium carbonate data of 0.75.

[14] The carbonate content is a bulk parameter influenced by marine productivity, dilution and dissolution and reflects a strong relationship with the number of foraminifera during the deglaciation and the Holocene outside the coast of northern Norway [*Knies et al.*, 2003]. The carbonate content in surface and cored sediments from the Nordic Seas is interpreted to reflect the influx of temperate Atlantic waters through time [*Kellogg*, 1976; *Ramm*, 1988; *Baumann et al.*, 1995; *Hebbeln et al.*, 1998; *Lackschewitz et al.*, 1998]. Throughout the northern North Atlantic and the Nordic Seas periods with high carbonate levels have been observed in records between 28 and 40 cal kyr B.P. [*Keigwig and Jones*, 1994; *Hagen and Hald*, 2002; *Moros et al.*, 2002; *Wilson and Austin*, 2002], associated with low percentages of *N. pachyderma* (s), indicating warmer surface waters [*Bond et al.*, 1992; *Hagen and Hald*, 2002; *Moros et al.*, 2002]. The Ca/Fe record of core MD99-2283 correlates strongly to GRIP [*Johnsen et al.*, 2001] (Figure 4) and sea surface temperatures in the northern North Atlantic [*van Kreveld et al.*, 2000]. The coupling between the Ca record and GRIP between 29 and 31 cal kyr B.P. shows that also smaller D-O type events can be observed in the records. The increase in carbonate associated with H2 was associated with a strong increase in the number of foraminifera in core MD99-2283, up to 900 foraminifera per gram of sediment. Similar findings from the Faroe-Shetland Channel [*Rasmussen et al.*, 1996, 1997] and the northern North Atlantic [*Lackschewitz et al.*, 1998] suggest increased productivity during this period.

[15] In core MD99-2283 the TOC record varies in complete antiphase with the carbonate record (Figure 4) and most likely reflects the amount of terrigenous organic material delivered from land during glacial times [*Villanueva et al.*, 1997; *Martrat et al.*, 2003]. This is confirmed by unpublished bulk sediment Rock-Eval pyrolisis, N_{inorg} and $\delta^{13}C$ measurements (J. Knies, unpublished data, 2005). Interstadials are marked by a lower TOC because of a reduced terrestric input, as was found in the North Atlantic [*Villanueva et al.*, 1997] and the TOC record provides independent support for the coupling of the records with interstadial-stadial changes in the North Atlantic region.

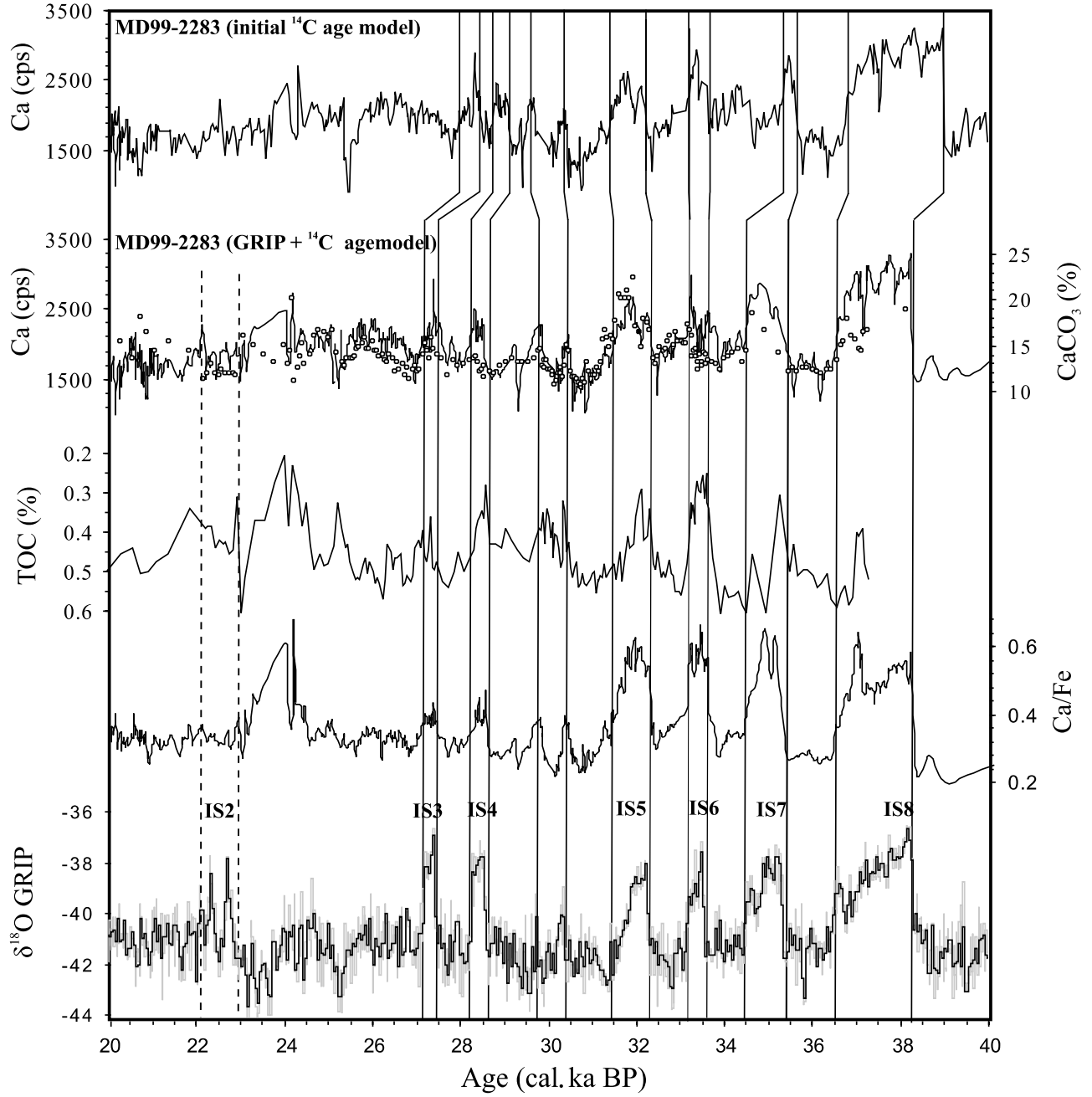

Figure 4. Correlation of the Ca, Ca/Fe, and total organic carbon (TOC) records of core MD99-2283 with the δ^{18}O record of the Greenland Ice Core Project (GRIP), using the ss09sea age scale [*Johnsen et al.*, 2001].

3.3. Sedimentology

[16] The upper 4 m of the core MD99-2283 are characterized by three broad spikes of coarse IRD (>2 mm), also reflected in the sand fractions larger then 63 and 150 μm and in the coarse chalk fraction >1 mm. Small amounts of coarse IRD are spread across the rest of the core (Figures 2 and 5). Large clasts between 5 and 10 cm were observed at 145, 225 and 605 cm, with the clast at 605 cm being very well rounded. Several smaller IRD events are recognized in the larger than 150 and 63 μm fractions and changes in grain size are partly reflected in the gamma ray density and quite strongly in the magnetic susceptibility record. Single chalk fragments larger then 1 mm occur in the record around 530, between 707 and 750 cm, around 935 and between 1278 and 1473 cm depth. The clay fraction makes up between 32% and 55% of the sediment and the silt fraction between 30% and 55%. The grain size distribution is polymodial and all samples contain more the 20% material smaller then 1 μm, indicating hemipelagic settling. The macrofaunal bioturbation identified from the X rays is of the *Mycellia*

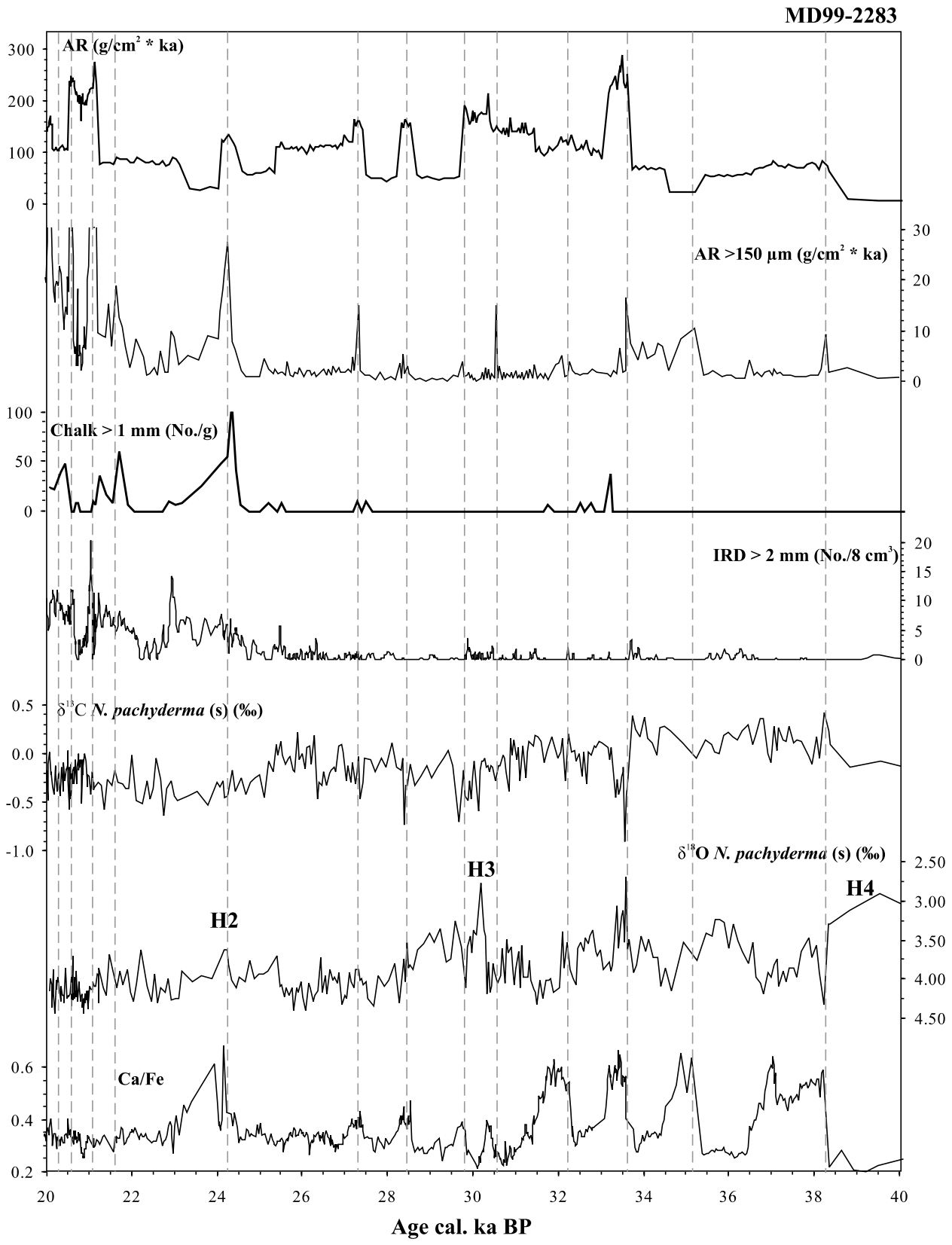

Figure 5. Accumulation rate (AR) of the fraction larger then 150 μm, number of chalk >1 mm, IRD >2 mm, oxygen and carbon isotope data measured on *N. pachyderma* (s), and Ca/Fe of core MD99-2283 between 20 and 40 cal kyr B.P. Dashed lines indicate IRD events based on the accumulation rate of the fraction >150 μm.

type, small filaments with a diameter of about 0.1 mm and a length ranging from one to several centimeters long [*Blanpied and Bellaiche*, 1981]. The amount of macrofaunal bioturbation is low and the intervals with increased bioturbation are associated with low amounts of IRD. Bioturbated zones of up to 15 cm were observed, which does not significantly affect the age model, considering the average sedimentation rate of 65 cm/kyr in the upper 14 m of the core.

[17] High concentrations of IRD > 2 mm and the presence of cobbles (Figure 2) in a hemipelagic environment are generally accepted as clear evidence for iceberg calving. Although gravel size clasts can be transported by sea ice and distal icebergs, studies on surface sediments [*Pirrung et al.*, 2002] and sediment cores [*Smith and Andrews*, 2000; *Knies et al.*, 2001] show a strong association of high concentrations of large clasts with the close presence of tidal glaciers or ice streams. *Dowdeswell and Elverhøi* [2002] showed that increased amounts of IRD >500 μm on the western Barents Sea margin are associated with the proximal advance and retreat of ice streams in the Barents Sea, while little IRD was observed during the maximum extension of the ice stream. The presence of coarse IRD on the edges of icebergs, lack of englacial coarse material and rapid release of ice rafted sediments within 200 km of the point of iceberg release [*Benn and Evans*, 1998; *Andrews*, 2000] would generally lead to a proximal deposition of coarse sediments. The three large increases in the different grain size parameters between 20 and 24 cal kyr B.P. seem to be the result of large amounts of calving in the immediate vicinity of the core site. The gradually coarsening upwards sequences further indicate that the dropstones are not the result from randomly passing icebergs [*Knies and Vogt*, 2003] and have only been observed in large numbers close to an ice margin [e.g., *Andrews and Principato*, 2002; *Dowdeswell and Elverhøi*, 2002; *Knies and Vogt*, 2003].

[18] The increased ice rafting observed at the core site after 25 cal kyr B.P. is associated with an active NCIS, as indicated from the observed large amounts of coarse chalk (Figure 5). The coarse ice rafted chalk fragments in this region are mainly derived from Cretaceous deposits in the North Sea and the south Baltic areas and reflect active erosion and iceberg calving of the NCIS [*Bischof et al.*, 1997; *Hebbeln and Wefer*, 1997; *King et al.*, 1998; *Berstad*, 2003], supporting the interpretation of proximity to iceberg calving during consistent periods with coarse IRD (>1 mm). During the period between 25 and 20 cal kyr B.P., increases in IRD have been observed in the Faroe-Shetland Channel [*Rasmussen et al.*, 1996], the central Norwegian Sea [*Bauch et al.*, 2001], the Vøring Plateau [*Dokken and Jansen*, 1999; *Berstad*, 2003] and the Denmark Strait [*Hagen and Hald*, 2002] indicating near simultaneous increased calving on the glaciated margins of the Nordic Seas. During the same time period, improving oceanic conditions are indicated by increases in the amount of planktonic foraminifera *Turborotalia quinqueloba* and of the benthic foraminifera *Cibicidoides wuellerstorfi* in the central Norwegian Sea [*Bauch et al.*, 2001], SST reconstruction in the Denmark Strait [*Hagen and Hald*, 2002], coccoliths and planktonic foraminifera in the northern North Atlantic [*Lackschewitz et al.*, 1998] and an increased reconstructed heat flux to the Nordic Seas between 21 and 24 cal kyr B.P. [*Weinelt et al.*, 2003]. The observed regional increase in IRD deposition from around 25 cal kyr B.P. in the Nordic Seas seem to reflect the maximal extension of the ice sheets together with increased heat flux to the Nordic Seas.

[19] The smaller spikes in the percentages of grains larger then 63 and 150 μm in core MD99-2283 are mainly siliciclastic. Since the fraction larger then 150 μm needs current speed above 70 cm/s 1 m above the seabed to be transported by currents [*Miller et al.*, 1977], non sorted increases in the medium to coarse sand fractions are interpreted as increased deposition from icebergs [e.g., *Heinrich*, 1988; *Hebbeln et al.*, 1998]. Both the grain size parameters and the AR rate of the fraction larger the 150 μm (Figure 5) display repetitive ice rafting events occurring prior to the rapid increased in Ca and Ca/Fe. This is in agreement with observation in the Irminger Basin and the Norwegian Sea [*Elliot et al.*, 1998; *van Kreveld et al.*, 2000], showing increased IRD during cold stadial and marking the transition to warmer climate. The observed IRD at the end of cold D-O stadial in core MD99-2283 probably represents a regional ice rafting signal similar to the multi sourced IRD signal documented in the Irminger Sea by hematite stained grains, ice rafted tephra and other ice rafted material [*van Kreveld et al.*, 2000].

3.4. Carbon Isotopes

[20] *N. pachyderma* (s) $\delta^{13}C$ measurements in core MD99-2283 fall between −1.0 and 0.5‰ and show no relation with the other proxy records of core MD99-2283. Strong depletion occurs between 34 and 33 kyr B.P., around 30, 28.5 and 27.5 kyr B.P. and between 25 and 20 kyr B.P. To compare the results of core MD99-2283 with the regional variability the result were plotted against the $\delta^{18}O$, together with averages of cores in the region (Figure 6). On the basis of this study and other core records the average glacial value of $\delta^{13}C$ measured on *N. pachyderma* (s) from the Nordic Seas between 20 and 40 cal kyr B.P. is calculated to 0.1 ± 0.2‰ (n = 1522) [*Sarnthein et al.*, 1995; *Dokken and Jansen*, 1999; *Dreger*, 1999; *van Kreveld et al.*, 2000; *Berstad*, 2003].

[21] When comparing $\delta^{13}C$ values with $\delta^{18}O$ values measured on modern and glacial *N. pachyderma* (s) from different sites in the Nordic and Arctic Seas (Figure 6), one can observe that known meltwater affected sites in the Eastern Fram Strait, the Laptev Sea, the glacial Arctic and the Vøring Plateau [*Spielhagen and Erlenkeuser*, 1994; *Bauch and Weinelt*, 1997; *Volkmann and Mensch*, 2001; *Spielhagen et al.*, 2004; *Lekens et al.*, 2005], have strongly negative $\delta^{13}C$ values compared to unaffected modern values of the Norwegian Sea [*Sarnthein et al.*, 1995]. However, a range of factors affect $\delta^{13}C$, like inflow and upwelling of $\delta^{13}C$ depleted water, low nutrient availability, productivity, large amount of terrigenous input and/or inflow of meltwater [e.g., *Bauch et al.*, 2001; *Volkmann and Mensch*, 2001; *Bauch et al.*, 2002], making it difficult to isolate the different influences.

[22] Since the foraminifera were picked for constant size and have an average weight around 10 μg, size differenti-

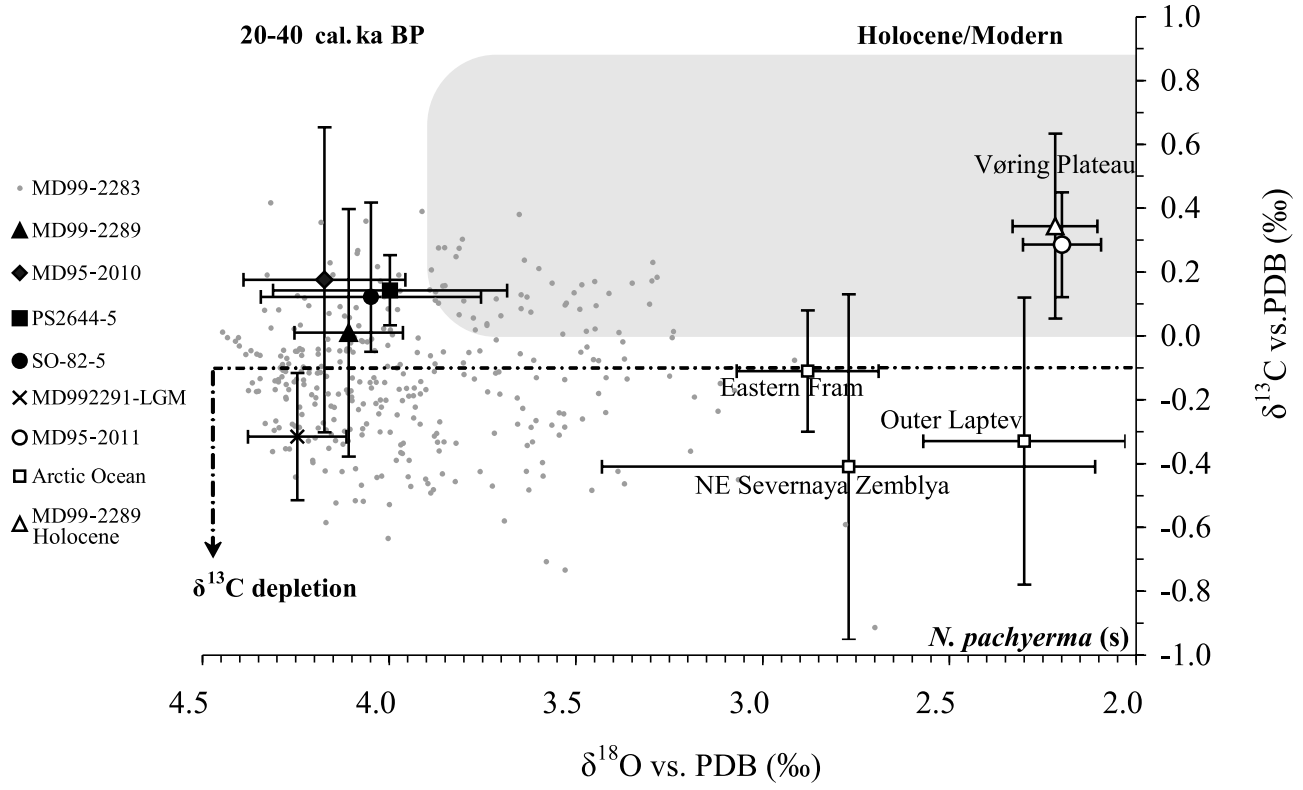

Figure 6. Oxygen and carbon isotope composition of *N. pachyderma* (s) in the Arctic and Nordic seas. Points with error bars represent mean values and associated standard deviations. Shaded area marks modern values in the Norwegian Sea [after *Sarnthein et al.*, 1995]. Data from MD99-2289 are by *Berstad* [2003], from MD99-2210 are by *Dokken and Jansen* [1999], from MD95-2212 are by *Dreger* [1999], from MD99-2291 are by *Lekens et al.* [2005], from SO82-05 are by *van Kreveld et al.* [2000], from PS2644-5 are by *Voelker et al.* [1998], and data from the Arctic Ocean are by *Volkmann and Mensch* [2001].

ation did probably not significantly affect the measurements [*Hillaire-Marcel et al.*, 2004]. To explain the observed depleted $\delta^{13}C$ values with the carbonate ion effect increases in the ocean carbonate concentrations of 50–100 μmol/kg are required [*Spero et al.*, 1997; *Bauch et al.*, 2002]. The latter seems unlikely in a glacial setting, since the carbonate ion effect causes oceanic $\delta^{13}C$ to rise with 0.11‰ per degree of temperature rise [*Mook et al.*, 1974; *Zhang et al.*, 1995]. In core MD99-2283 carbonate productivity seems to be unrelated to changes in $\delta^{13}C$, which is similar to observation in the Arctic Ocean during the last 200 kyr [*Spielhagen et al.*, 2004], but more direct evidence is needed to assess productivity. On the basis of the available data set from the Nordic Seas, it is suggested that the glacial $\delta^{13}C$ of the surface waters is mostly affected by the combined influence of reduced surface water mixing and meltwater input.

3.5. Oxygen Isotopes

[23] The $\delta^{18}O$ values in core MD99-2283 measured on *N. pachyderma* (s) vary from 2.8 to 4.4‰, with strong light spikes associated with H3 at 8.02 m, around 11.50 m and associated with H4 at 13.87 m depth (Figure 2). These large meltwater anomalies seem to occur all around the Nordic Seas, close to glaciated margins (Figures 7 and 8) and might be delivered by melting icebergs [e.g., *Cortijo et al.*, 1997], sudden input of fresh water [e.g., *Spielhagen et al.*, 2004] or by the circulation of distal fresh water pulses [e.g., *Belkin et al.*, 1998]. Significant meltwater anomalies in the record are characterized by $\delta^{18}O$ anomalies larger then 0.5‰ together with $\delta^{13}C$ values lower then −0.1‰ versus VPDB, both measured on *N. pachyderma* (s).

[24] The large anomaly associated with H4 in core MD99-2283 is devoid of significant amounts of IRD and was observed with an even larger amplitude on the northern Faroe Margin [*Rasmussen et al.*, 1996]. While no clear source for the meltwater has been identified in the area some evidence for fresh water trapping exists. Subglacial meltwater was shown to be trapped in the Skjonhelleren cave during H4 between the Laschamp event and the start of D-O event 8 [*Mangerud et al.*, 2003] and during approximately the same period lacustrine deposits are observed in Denmark suggesting dammed lakes [*Houmark-Nielsen and Kjaer*, 2003]. The $\delta^{18}O$ spike observed around H4 is also locally expressed outside the Bear Island Through, on the Vøring Plateau (Figures 7 and 8) and in the Denmark Strait [*Voelker et al.*, 1998; *Dokken and Jansen*, 1999; *Dreger*, 1999]. While restricted by the number of observations the lateral extent of the observed meltwater spikes in the Nordic

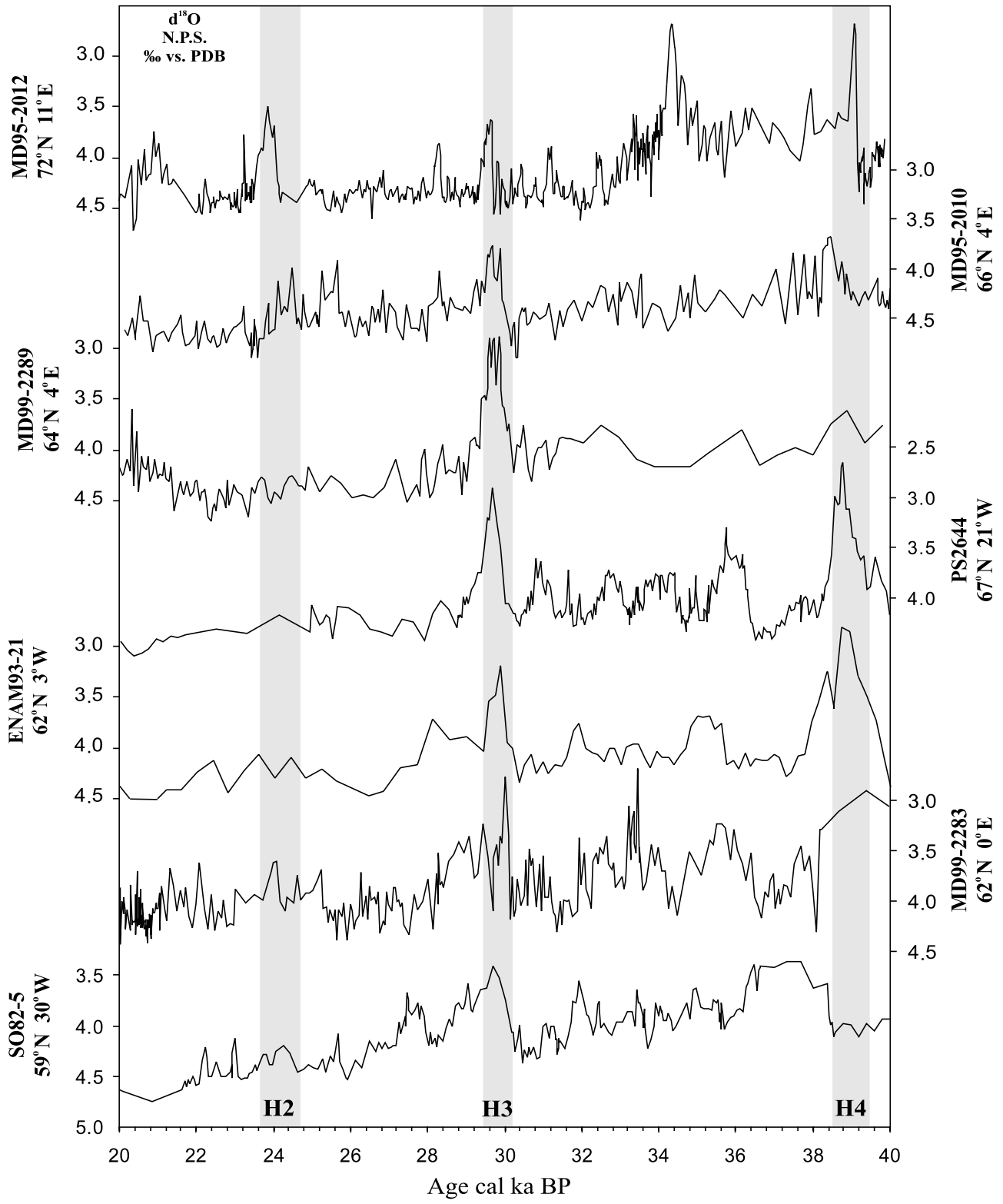

Figure 7. The $\delta^{18}O$ records from the Nordic Seas and the North Atlantic measured on *N. pachyderma* (s). Data are after *Berstad* [2003], *Dokken and Jansen* [1999], *Dreger* [1999], *Rasmussen et al.* [1996], *Rasmussen and Thomsen* [2004], *van Kreveld et al.* [2000], and *Voelker et al.* [1998]. H4 was used as a tie point in the age models of cores MD95-2012 and ENAM93-21 based on *Rasmussen et al.* [1996] and *Dreger* [1999].

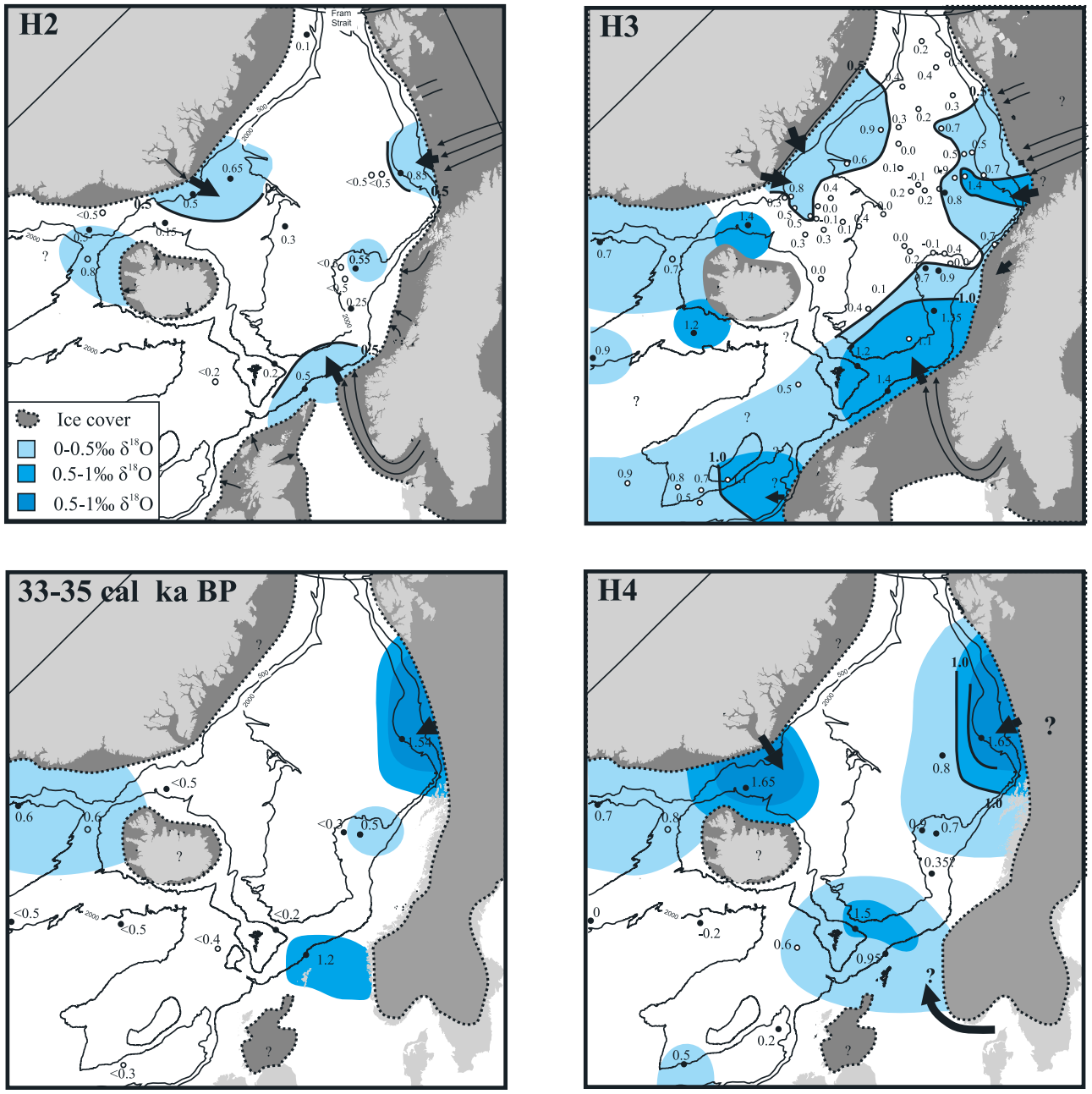

Figure 8. Distribution of $\delta^{18}O$ anomalies in the Nordic Seas during Heinrich events and between 33 and 35 cal kyr B.P. (difference between $\delta^{18}O$ before event and at the $\delta^{18}O$ at height of the event) measured on *N. pachyderma* (s). The global ice volume and temperature effects are not subtracted from the isotope data. Data are after *Andrews et al.* [1998], *Berstad* [2003], *Dokken and Jansen* [1999], *Dreger* [1999], *Nam* [1997], *Rasmussen et al.* [1996], *van Kreveld et al.* [2000], *Vidal et al.* [1997], and *Voelker et al.* [1998]. Open circles denote estimated data from *Elliot et al.* [1998], *Hagen and Hald* [2002], *Rasmussen et al.* [2002], and *Sarnthein et al.* [1995, 2001].

Sea are smaller compared to the extent of the H4 meltwater anomaly in the North Atlantic [*Cortijo et al.*, 1997], modeled to be corresponding to a fresh water release of 2 ± 1 m of equivalent sea level [*Roche et al.*, 2004]. The observed anomalies are nevertheless associated with significant amounts of meltwater and contribute to the predicted 15 m sea level increase, originating in the Northern Hemisphere during H4 [*Rohling et al.*, 2004].

[25] Large $\delta^{18}O$ spikes were observed between 33 and 35 cal kyr B.P. on the northern North Sea margin, outside the Bear Island Trough [*Dreger*, 1999; *Sarnthein et al.*, 2001] and in the Irminger Basin [*Elliot et al.*, 1998; *Hagen and Hald*, 2002]. On the basis of the current age models

these light isotopic events are not synchronous and might be associated with local ice sheet changes. In Fennoscandia this period coincides with the end of a large glacial phase called the Valderøy stadial and meltwater deposits in caves [*Mangerud et al.*, 2003]. Radiocarbon dated laminated meltwater plume deposits observed at Jæren, southwestern Scandinavia [*Raunholm et al.*, 2003] also indicate that southern Fennoscandia contributed meltwater to the Nordic Seas during this time period and might explain the observed meltwater anomaly on the northern North Sea margin.

[26] The $\delta^{18}O$ spikes associated with H3 show the lightest values in the southeastern Norwegian Sea in core MD99-2283 and MD99-2289 (Figure 6 and 8), denoting the southern Fennoscandian ice sheet as a significant meltwater source. Dropstones and chalk fragments >1 mm in core MD99-2283 and chalk fragments observed in core MD99-2289 by *Berstad* [2003] indicate iceberg output from the NCIS during H3. However, the accumulation rate of the IRD during Heinrich event 3 is low in the southern Norwegian Sea [see also *Rasmussen et al.*, 1997]. The lack of large amounts of IRD during this period in core MD99-2283 and ENAM93-21 indicates that the fresh water signal is probably not due to the melting of icebergs, but rather to direct output of large amounts of fresh water.

[27] Some smaller meltwater events seem to have occurred in the Norwegian Sea between 30 and 28 cal kyr B.P. associated with D-O events 3 and 4 (Figure 7). No clear source for these spikes can be assigned. However, around 29 cal kyr B.P. an ice retreat occurred in Scandinavia denoted as the Hamnsund interstadial [*Valen et al.*, 1996], possibly leading to the release of smaller amounts of meltwater along the Norwegian margin. The light isotope spikes between 25 and 26 cal kyr B.P., prior to H2 are prominent in MD99-2283, MD95-2010 and potentially also in MD95-2012 (Figure 7). These and other small $\delta^{18}O$ spikes seem to be local and not associated with large amounts of warm water inflow to the Nordic Seas [*Weinelt et al.*, 2003], clear interstadials on land or significant ice rafting. During the same time $\delta^{18}O$ spikes have been observed with a lesser amplitude in the Labrador Sea, just outside the Hudson Strait [*Andrews et al.*, 1994] and in the northern North Atlantic [*van Kreveld et al.*, 2000; *Rasmussen et al.*, 2003]. Oxygen isotope records outside the Scoresby Sund also suggest that eastern Greenland might have been a source area for meltwater during this period [*Funder et al.*, 1998]. While no causal relation is apparent, the small $\delta^{18}O$ spikes seem to be a common feature of ice margins around the Nordic Seas during full glacial conditions. If not because of measurement error or problems with the planktonic foraminifera the spikes might indicate small episodic releases of meltwater by the ice margin, not necessarily related to climatic changes.

[28] During H2 isolated $\delta^{18}O$ spikes in core MD99-2283 and especially in front of the Bear Island Through indicate significant meltwater outflow from these parts of the Fennoscandian ice sheet. However, significant spikes were observed in association with H2 in the northern part of the Denmark Strait [*Andrews et al.*, 1998; *van Kreveld et al.*, 2000] and the central Norwegian Sea [*Bauch et al.*, 2001], but they were clearly observed south of Iceland [*Hagen and Hald*, 2002] and along the southeastern coast of Greenland [*Elliot et al.*, 2001]. The lack of $\delta^{18}O$ spikes associated with the period before and during H2 in the central Norwegian Sea [*Bauch et al.*, 2001] indicates that the spikes remained local; suggest limited surface circulation and indicate a more limited meltwater production in the Nordic Seas during H2 then during H3 and H4.

[29] When comparing the meltwater history of the Norwegian Sea with that of the Labrador Sea and the North Atlantic some clear differences can be observed. While meltwater in the North Atlantic during Heinrich events is associated with large increases in ice rafting, the meltwater spikes in the southern Norwegian Sea are not always associated with increases in IRD. Also the occurrence of large amounts of IRD is not reflected in the planktonic $\delta^{18}O$ record. This suggests ''clean'' icebergs [e.g., *Andrews*, 2000] or subglacial meltwater release in the Nordic Seas. On the basis of the lateral extent and the amplitude of the light isotopic events, individual meltwater anomalies during Heinrich events seemed to have been limited compared to those observed in the North Atlantic. The observed geographically confined meltwater spikes and the steep isotopic gradients (Figure 6 and 8) in different areas of the Nordic Seas [see also *Sarnthein et al.*, 1995], indicate reduced surface water circulation and limited mixing during these events. The meltwater spikes between 34 and 36 cal kyr B.P. also demonstrates the possibility of major meltwater release during interstadials.

3.6. Regional Implications

[30] Within the uncertainties of the dating tools, the perceived synchronicity of the multisourced material associated with the D-O and Heinrich events [*Bond et al.*, 1997; *van Kreveld et al.*, 2000], indicates glacial and climatic reorganizations on an ocean-wide scale and a common trigger mechanism. Recently, intrusions of Atlantic intermediate waters have been suggested to explain changes in the benthic foraminiferal assemblage and benthic isotope signals in the Nordic Seas [*Bauch et al.*, 2001; *Rasmussen et al.*, 2002; *Rasmussen and Thomsen*, 2004]. Slight increases in the amount of warm planktonic foraminifera [*Sarnthein et al.*, 2001; *Weinelt et al.*, 2003] might suggest an increased heat transport to the north at the end of cold D-O events. Model experiments have shown that such subsurface heat in the Nordic Seas would be able to produce a D-O type climatic signal and destabilize the ice shelves [*Hulbe et al.*, 2004; *Shaffer et al.*, 2004]. The observed meltwater pooling in the Nordic Seas would play an important role in such a model, creating a meltwater lid and trapping heat in the deeper water masses of the Nordic Seas, as also shown by the model of *Knutti et al.* [2004]. The occurrence of meltwater and IRD on the northern North Sea margin at the end of non-Heinrich, stadial phases suggests that the icebergs and meltwater occur in a reaction to outside forcing rather then trigger D-O events [see also *van Kreveld et al.*, 2000]. The observed association of the IRD with the rapid increases in Ca content, independent from age models or other inferences, suggests a strong relation to inflow of warm Atlantic waters.

[31] The large meltwater spikes observed in this study are not associated with strong surface warming in the Nordic Seas [*van Kreveld et al.*, 2000; *Sarnthein et al.*, 2001; *Weinelt et al.*, 2003]. As such, direct melting of ice sheets and margins probably played a minor contribution. Neither are the meltwater anomalies associated with large amounts of IRD, limiting the role of meltwater input through iceberg melting, although sediment free ice could make a significant unknown contribution. It seems likely that the sudden release of ice-dammed lakes and subglacially trapped meltwater was responsible for much of the observed meltwater anomalies on the eastern side of the Nordic Seas. The occurrence of meltwater anomalies near known former large ice streams [*Vorren and Laberg*, 1997], seems to support this hypotheses since these areas would provide the natural conduits for trapped meltwater and would be very susceptible to environmental changes [e.g., *Dowdeswell and Elverhøi*, 2002; *Joughin et al.*, 2004; *Lekens et al.*, 2005].

[32] The near simultaneous occurrence of large meltwater anomalies during H events in different corners of the Nordic Seas, the North Atlantic and around Antarctica is potentially linked by increases in sea level during these events. The observed sea level rises of over 30 m, associated with H events during MIS3 and MIS2 [*Chappell*, 2002; *Siddall et al.*, 2003; *Rohling et al.*, 2004], would cause increased calving along the ice margin [*Hughes*, 2002] and destabilize ice dams. This could subsequently lead to the draining of ice-dammed lakes, causing localized large outburst of fresh water. As such a direct coupling between meltwater release from the northern ice sheets and Antarctica is possible through sea level forcing, and seems related to the warming in the Southern Hemisphere [*Rohling et al.*, 2004]. As such the delivery of meltwater in the Nordic Seas would provide an important feedback mechanism to increasing sea level. However, the large local meltwater anomalies between 33 and 35 cal kyr B.P. and H2 are not related to any observed sea level changes [*Lambeck and Chappell*, 2001; *Siddall et al.*, 2003]. On the other hand, the events between 33 and 35 cal kyr B.P. observed in the Nordic Seas do not appear to be synchronous, suggesting an independent mechanism. Meltwater and/or iceberg outbursts purely driven by internal mechanisms of the ice sheet [e.g., *Alley and MacAyeal*, 1994; *Geirsdottir et al.*, 2000] seems to be a most likely mechanism for the events around 34 cal kyr B.P. occur and cannot be excluded as a trigger mechanism for the other events.

4. Conclusions

[33] The southern Norwegian Sea shows clear signs of both meltwater and IRD release between 40 and 20 cal kyr B.P. originating from the southern Fennoscandian ice sheet, confirmed by the presence of localized meltwater anomalies and the deposition of coarse chalk. Within the core record the period between 40 and 24 cal kyr B.P. is characterized by distinct D-O cyclicity with the carbonate record following temperature changes in the region and IRD occurring right before sharp climatic improvements. The observed regional increase in IRD deposition after 25 cal kyr B.P. in the Nordic Seas seems to reflect the maximum extension of the ice sheets together with increased heat flux to the Nordic Seas.

[34] Local meltwater spikes have been observed in the Norwegian Sea during Heinrich events and between 33 and 35 cal kyr B.P. The absence of these spikes in several high-resolution records in the Norwegian Sea indicates local pooling of meltwater and limited surface circulation and mixing in the Norwegian Sea during periods of meltwater release. Using a paleogeographic reconstruction of the available oxygen isotope data it can be shown that the NCIS area, the Bear Island ice stream, the East Greenland ice streams and potentially Iceland were sources of meltwater during Heinrich events 2, 3 and 4 and between 33 and 35 cal kyr B.P. Prior to H2, a smaller meltwater event was observed in the southern Norwegian Sea possibly associated with a retreat of ice in the central North Sea.

[35] The geographic distribution of the meltwater anomalies and the provenance data in the Norwegian Sea points to the northern North Sea and the Barents Sea as important European meltwater and sediment contributors during Heinrich events. The localized meltwater spikes in the southern Norwegian Sea are associated with limited IRD, suggesting that the primary source of the meltwater is not the icebergs themselves but related to a sudden release of meltwater. The draining of confirmed large freshwater lakes and large amounts of subglacial meltwater in the region may have caused these events. The simultaneous occurrence of localized meltwater discharge during Heinrich events indicates an external common triggering mechanism, presumably related to the large sea level increases during these periods.

[36] **Acknowledgments.** This research was funded by a scholarship of the Research Council of Norway (RCN) and is a contribution to the RCN project NORPAST-2. Magnetic measurements on U channels were performed at the facilities of the University of Bremen and funded by EU Project "Paleostudies," contract HPRI-CT-2001-0124. We wish to thank T. Frederichs for his help with the magnetic measurements. The U channels used in this study were designed and developed at the Paleomagnetism and Environmental Magnetism Laboratory of the LSCE, Gif-sur-Yvette. We wish to thank T. P. Allaway for the help with the X rays and grain-size analysis and U. Ninnemann and R. Søraas for their comments, supervision, and instructions concerning the isotope analysis. The crew of the *Marion Dufresne* is thanked for the recovery of core MD99-2283. We wish to thank R. Løvlie, C. Vogt, and three anonymous reviewers for their comments on the manuscript.

References

Alley, R. B., and D. R. MacAyeal (1994), Ice-rafted debris associated with binge/purge oscillations of the Laurentide ice sheet, *Paleoceanography*, *9*, 503–511.

Andrews, J. T. (2000), Icebergs and iceberg rafted detritus (IRD) in the North Atlantic: Facts and assumptions, *Oceanography*, *13*, 100–108.

Andrews, J. T., and S. M. Principato (2002), Grain-size characteristics and provenance of ice-proximal glacial marine sediments, in *Glacier-Influenced Sedimentation on High-*

Latitude Continental Margins, edited by J. A. Dowdeswell and C. O. Cofaigh, pp. 305–324, Geol. Soc. of London, London.

Andrews, J. T., H. Erlenkeuser, K. Tedesco, A. E. Aksu, and A. J. T. Jull (1994), Late Quaternary (stage 2 and 3) meltwater and Heinrich events, northwest Labrador Sea, *Quat. Res.*, *41*, 26–34.

Andrews, J. T., T. A. Cooper, A. E. Jennings, A. B. Stein, and H. Erlenkeuser (1998), Late Quaternary iceberg-rafted detritus events on the Denmark Strait–southeast Greenland continental slope (~65°N): Related to North Atlantic Heinrich events?, *Mar. Geol.*, *149*, 211–228.

Auffret, G., S. Zaragosi, B. Dennielou, E. Cortijo, R. D. van, F. Grousset, C. Pujol, F. Eynaud, and M. J. Siegert (2002), Terrigenous fluxes at the Celtic margin during the last glacial cycle, *Mar. Geol.*, *188*, 79–108.

Austin, W. E. N., E. Bard, J. B. Hunt, D. Kroon, and J. D. Peacock (1995), The ^{14}C age of the Icelandic Vedda ash: Implications for the Younger Dryas marine reservoir age corrections, *Radiocarbon*, *37*, 53–62.

Barber, D. C., et al. (1999), Forcing of the cold event of 8,200 years ago by catastrophic drainage of Laurentide lakes, *Nature*, *400*, 344–348.

Bard, E. (1988), Correction of accelerator mass spectrometry ^{14}C ages measured in planktonic foraminifera: Paleoceanographic implications, *Paleoceanography*, *3*, 635–645.

Bard, E., M. Arnold, J. Mangerud, M. Paterne, L. Labeyrie, J. Duprat, M. A. Melieres, E. Sonstegaard, and J. C. Duplessy (1994), The North Atlantic atmosphere-sea surface ^{14}C gradient during the Younger Dryas climatic event, *Earth. Planet. Sci. Lett.*, *126*, 275–287.

Bauch, H. A., and M. S. Weinelt (1997), Surface water changes in the Norwegian Sea during last deglacial and Holocene times, *Quat. Sci. Rev.*, *16*, 1115–1124.

Bauch, H. A., H. Erlenkeuser, R. F. Spielhagen, U. Struck, J. Matthiessen, J. Thiede, and J. Heinemeier (2001), A multiproxy reconstruction of the evolution of deep and surface waters in the subarctic Nordic seas over the last 30,000 yr, *Quat. Sci. Rev.*, *20*, 659–678.

Bauch, D., H. Erlenkeuser, G. Winckler, G. Pavlova, and J. Thiede (2002), Carbon isotopes and habitat of polar planktic foraminifera in the Okhotsk Sea: The "carbonate ion effect" under natural conditions, *Mar. Micropaleontol.*, *45*, 83–99.

Baumann, K.-H., K. S. Lackschewitz, J. Mangerud, R. F. Spielhagen, T. C. W. Wolf-welling, R. Henrich, and H. Kassens (1995), Reflection of Scandinavian ice sheet fluctuations in Norwegian Sea sediments during the past 150,000 years, *Quat. Res.*, *43*, 185–197.

Belkin, I. M., S. Levitus, J. Antonov, and S.-A. Malmberg (1998), "Great Salinity Anomalies" in the North Atlantic, *Prog. Oceanogr.*, *41*, 1–68.

Benn, D. I., and D. J. A. Evans (1998), *Glaciers and Glaciation*, 734 pp., Edward Arnold, London.

Berger, W. H., and U. von Rad (2002), Decadal to millennial cyclicity in varves and turbidites from the Arabian Sea: Hypothesis of tidal origin, *Global Planet. Change*, *34*, 313–325.

Berger, W. H., J. Paetzold, and G. Wefer (2002), A case for climate cycles: Orbit, Sun and Moon, in *Climate Development and History of the North Atlantic Realm*, pp. 101–123, Springer, New York.

Berstad, I. M. (2003), Quaternary climate variability in the eastern Nordic Sea region inferred from speleothems and deep-sea cores, Ph.D. thesis, 140 pp., Univ. of Bergen, Bergen, Norway.

Best, A. I., and D. E. Gunn (1999), Calibration of marine sediment core loggers for quantitative acoustic impedance studies, *Mar. Geol.*, *160*, 137–146.

Bischof, J., J. J. Lund, and H. H. Ecke (1997), Palynomorphs of ice rafted clastic sedimentary rocks in late Quaternary glacial marine sediments of the Norwegian Sea as provenance indicators, *Palaeogeogr. Palaeoclimatol. Palaeoecol.*, *129*, 329–360.

Björck, S., N. Koc, and G. Skog (2003), Consistently large marine reservoir ages in the Norwegian Sea during the last deglaciation, *Quat. Sci. Rev.*, *22*, 429–435.

Blais-Stevens, A., J. J. Clague, R. W. Mathewes, R. J. Hebda, and B. D. Bornhold (1981), Record of large, late Pleistocene outburst floods preserved in Saanich Inlet sediments, Vancouver Island, Canada, *Quat. Sci. Rev.*, *22*, 23272003.

Blanpied, C., and G. Bellaiche (1981), Bioturbation on the Pelagian Platform: Ichnofacies variations as palaeoclimatic indicator, *Mar. Geol.*, *43*, M49–M57.

Bond, G. C., et al. (1992), Evidence for massive discharges of icebergs into the North Atlantic ocean during the last glacial period, *Nature*, *360*, 245–249.

Bond, G. C., W. Broecker, S. Johnsen, J. McManus, L. Labeyrie, J. Jouzel, and G. Bonani (1993), Correlations between climate records from North Atlantic sediments and Greenland ice, *Nature*, *365*, 143–147.

Bond, G., W. J. Showers, M. Cheseby, R. Lotti, P. Almasi, P. deMenocal, P. Priore, H. Cullen, I. Hajdas, and G. Bonani (1997), A pervasive millennial-scale cycle in North Atlantic Holocene and glacial climates, *Science*, *278*, 1257–1266.

Broecker, W. S., G. Bond, M. Klas, G. Bonani, and W. Wolfli (1990), A salt oscillator in the glacial Atlantic? 1. The concept, *Paleoceanography*, *5*, 469–477.

Broecker, W. S., G. C. Bond, M. Klas, E. A. Clark, and J. McManus (1992), Origin of the northern Atlantic's Heinrich events, *Clim. Dyn.*, *6*, 265–273.

Chappell, J. (2002), Sea level changes forced ice breakouts in the last glacial cycle: New results from coral terraces, *Quat. Sci. Rev.*, *21*, 1229–1240.

Clark, C. D., D. J. A. Evans, A. Khatwa, T. Bradwell, C. J. Jordan, S. H. Marsh, W. A. Mitchell, and M. D. Bateman (2004), Map and GIS database of glacial landforms and features related to the last British ice sheet, *Boreas*, *33*, 359–375.

Claussen, M., A. Ganopolski, V. Brovkin, F.-W. Gerstengarbe, and P. Werner (2003), Simulated global-scale response of the climate system to Dansgaard/Oeschger and Heinrich events, *Clim. Dyn.*, *21*, 361–370, doi:310.1007/s00382-00003-00336-00382.

Cortijo, E., L. Labeyrie, L. Vidal, M. Vautravers, M. Chapman, J. C. Duplessy, M. Elliot, M. Arnold, J. L. Turon, and G. Auffret (1997), Changes in sea surface hydrology associated with Heinrich event 4 in the North Atlantic Ocean between 40° and 60°N, *Earth Planet. Sci. Lett.*, *146*, 29–45.

Dokken, T., and E. Jansen (1999), Rapid changes in the mechanism of ocean convection during the last glacial period, *Nature*, *401*, 458–461.

Dowdeswell, J. A., and A. Elverhøi (2002), The timing of initiation of fast-flowing ice streams during a glacial cycle inferred from glacimarine sedimentation, *Mar. Geol.*, *188*, 3–14.

Draut, A. E., M. E. Raymo, J. F. McManus, and D. W. Oppo (2003), Climate stability during the Pliocene warm period, *Paleoceanography*, *18*(4), 1078, doi:10.1029/2003PA000889.

Dreger, D. (1999), Decadal-to-centennial-scale sediment records of ice advance on the Barents shelf and meltwater discharge into the northeastern Norwegian Sea over the last 40 kyr, Ph.D. thesis, 71 pp., Univ. of Kiel, Kiel, Germany.

Ehrmann, W. U., and J. Thiede (1986), Correlation of terrigenous and biogenic sediment fluxes in the North Atlantic Ocean during the past 150 my, *Geol. Rund.*, *75*, 43–55.

Elliot, M., L. Labeyrie, G. Bond, E. Cortijo, J. L. Turon, N. Tisnerat, and J. C. Duplessy (1998), Millennial-scale iceberg discharges in the Irminger Basin during the last glacial period: Relationship with the Heinrich events and environmental settings, *Paleoceanography*, *13*, 433–446.

Elliot, M., L. Labeyrie, T. Dokken, and S. Manthe (2001), Coherent patterns of ice-rafted debris deposits in the Nordic regions during the last glacial (10–60 ka), *Earth Planet. Sci. Lett.*, *194*, 151–163.

Fairbanks, R. G., R. A. Mortlock, T.-C. Chiu, L. Cao, A. Kaplan, T. P. Guilderson, T. W. Fairbanks, A. L. Bloom, P. M. Grootes, and M.-J. Nadeau (2005), Radiocarbon calibration curve spanning 0 to 50,000 years BP based on paired ^{230}Th/^{234}U/^{238}U and ^{14}C dates on pristine corals, *Quat. Sci. Rev.*, *24*, 1781–1796.

Funder, S., C. Hjort, J. Y. Landvik, S. I. Nam, N. Reeh, and R. Stein (1998), History of a stable ice margin: East Greenland during the middle and upper Pleistocene, *Quat. Sci. Rev.*, *17*, 77–123.

Ganopolski, A., and S. Rahmstorf (2001), Rapid changes of glacial climate simulated in a coupled climate model, *Nature*, *409*, 153–158, doi:110.1038/35051500.

Geirsdottir, A., J. Hardardottir, and A. E. Sveinbjornsdottir (2000), Glacial extent and catastrophic meltwater events during the deglaciation of southern Iceland, *Quat. Sci. Rev.*, *19*, 1749–1761.

Grachev, A. M., and J. P. Severinghaus (2005), A revised +10 +4°C magnitude of the abrupt change in Greenland temperature at the Younger Dryas termination using published GISP2 gas isotope data and air thermal diffusion constants, *Quat. Sci. Rev.*, *24*, 513–519.

Grobe, H. (1987), A simple method for the determination of ice-rafted debris in sediment cores, *Polarforschung*, *57*, 123–126.

Grootes, P. M., and M. Stuiver (1997), Oxygen 18/16 variability in Greenland snow and ice with 10^3- to 10^5-year time resolution, *J. Geophys. Res.*, *102*, 26,455–26,470.

Guillou, H., B. S. Singer, C. Laj, C. Kissel, S. Scaillet, and B. R. Jicha (2004), On the age of the Laschamp geomagnetic excursion, *Earth Planet. Sci. Lett.*, *227*, 331–343.

Haflidason, H., H. P. Sejrup, D. K. Kristensen, and S. Johnson (1995), Coupled response of the late glacial climatic shifts of the northwest Europe reflected in Greenland ice cores: Evidence from the northern North Sea, *Geology*, *23*, 1059–1062.

Hagen, S., and M. Hald (2002), Variation in surface and deep water circulation in the Denmark Strait, North Atlantic, during marine isotope stages 3 and 2, *Paleoceanography*, *17*(4), 1061, doi:10.1029/2001PA000632.

Hall, I. R., and I. N. McCave (2000), Palaeocurrent reconstruction, sediment and thorium focussing on the Iberian margin over the last 140 ka, *Earth. Planet. Sci. Lett.*, *178*, 151–164.

Hebbeln, D., and G. Wefer (1997), Late Quaternary paleoceanography in the Fram Strait, *Paleoceanography*, *12*, 65–78.

Hebbeln, D., R. Henrich, and K. H. Baumann (1998), Paleoceanography of the last interglacial/glacial cycle in the polar North Atlantic, in *Glacial and Oceanic History of the Polar North Atlantic Margins*, pp. 125–153, Elsevier, New York.

Heinrich, H. (1988), Origin and consequences of cyclic ice rafting in the northeast Atlantic Ocean during the past 130,000 years, *Quat. Res.*, *29*, 142–152.

Helmke, J. P., H. A. Bauch, U. Rohl, and A. Mazaud (2005), Changes in sedimentation patterns of the Nordic seas region across the mid-Pleistocene, *Mar. Geol.*, *215*, 107–122.

Hillaire-Marcel, C., A. de Vernal, L. Polyak, and D. Darby (2004), Size-dependent isotopic composition of planktic foraminifers from Chukchi Sea vs. NW Atlantic sediments—Implications for the Holocene paleoceanography of the western Arctic, *Quat. Sci. Rev.*, *23*, 245–260.

Hopkins, T. S. (1991), The GIN Sea: A synthesis of its physical oceanography and literature review 1972–1985, *Earth Sci. Rev.*, *30*, 175–318.

Houmark-Nielsen, M., and K. H. Kjaer (2003), Southwest Scandinavia, 40–15 kyr BP: Palaeogeography and environmental change, *J. Quat. Sci.*, *18*, 769–786.

Hughen, K., S. Lehman, J. Southon, J. Overpeck, O. Marchal, C. Herring, and J. Turnbull (2004), ^{14}C activity and global carbon cycle changes over the past 50,000 years, *Science*, *303*, 202–207.

Hughes, T. J. (2002), Calving bays, in *Ice Sheets and Sea Level of the Last Glacial Maximum*, pp. 267–282, Elsevier, New York.

Hulbe, C. L., D. R. MacAyeal, G. H. Denton, J. Kleman, and T. V. Lowell (2004), Catastrophic ice shelf breakup as the source of Heinrich event icebergs, *Paleoceanography*, *19*, PA1004, doi:10.1029/2003PA000890.

Jansen, J. H. F., S. J. Van der Gaast, B. Koster, and A. J. Vaars (1998), CORTEX, a shipboard XRF-scanner for element analyses in split sediment cores, *Mar. Geol.*, *151*, 143–153.

Johnsen, S. J., D. Dahl-Jensen, N. Gundestrup, J. P. Steffensen, H. B. Clausen, H. Miller, V. Masson-Delmotte, A. E. Sveinbjörnsdottir, and J. White (2001), Oxygen isotope and palaeotemperature records from six Greenland ice-core stations: Camp Century, Dye-3, GRIP, GISP2, Renland and NorthGRIP, *J. Quat. Sci.*, *16*, 299–307.

Joughin, I., W. Abdalati, and M. Fahnestock (2004), Large fluctuations in speed on Greenland's Jakobshavn Isbrae glacier, *Nature*, *432*, 608–610.

Kanfoush, S. L., D. A. Hodell, C. D. Charles, T. P. Guilderson, P. G. Mortyn, and U. S. Ninnemann (2000), Millennial-scale instability of the Antarctic ice sheet during the last glaciation, *Science*, *288*, 1815–1818.

Kaspi, Y., R. Sayag, and E. Tziperman (2004), A "triple sea-ice state" mechanism for the abrupt warming and synchronous ice sheet collapses during Heinrich events, *Paleoceanography*, *19*, PA3004, doi:10.1029/2004PA001009.

Keigwig, L. D., and G. A. Jones (1994), Western North Atlantic evidence for millennial-scale changes in ocean circulation and climate, *J. Geophys. Res.*, *99*, 12,397–12,410.

Kellogg, T. (1976), Late Quaternary climatic changes: Evidence from deep-sea cores of Norwegian and Greenland seas, *Mem. Geol. Soc. Am.*, *145*, 77–110.

King, E. L., H. Haflidason, H. P. Sejrup, and R. Lovlie (1998), Glacigenic debris flows on the North Sea Trough Mouth Fan during ice stream maxima, *Mar. Geol.*, *152*, 217–246.

Kissel, C., C. Laj, L. Labeyrie, T. Dokken, A. Voelker, and D. Blamart (1999), Rapid climatic variations during marine isotopic stage 3: Magnetic analysis of sediments from Nordic Seas and North Atlantic, *Earth Planet. Sci. Lett.*, *171*, 489–502.

Knies, J., and C. Vogt (2003), Freshwater pulses in the eastern Arctic Ocean during Saalian and Early Weichselian ice-sheet collapse, *Quat. Res.*, *60*, 243–251.

Knies, J., H. P. Kleiber, J. Matthiessen, C. Mueller, and N. R. Nowaczyk (2001), Marine ice-rafted debris records constrain maximum extent of Saalian and Weichselian ice-sheets along the northern Eurasian margin, *Mar. Geol.*, *31*, 45–64.

Knies, J., M. Hald, H. Ebbesen, U. Mann, and C. Vogt (2003), A deglacial–middle Holocene record of biogenic sedimentation and paleoproductivity changes from the northern Norwegian continental shelf, *Paleoceanography*, *18*(4), 1096, doi:10.1029/2002PA000872.

Knutti, R., J. Flückiger, T. F. Stocker, and A. Timmermann (2004), Strong hemispheric coupling of glacial climate through freshwater discharge and ocean circulation, *Nature*, *430*, 851–856.

Lackschewitz, K. S., K. H. Baumann, B. Gehrke, A. H. J. Wallrabe, J. Thiede, G. Bonani, R. Endler, H. Erlenkeuser, and J. Heinemeier (1998), North Atlantic ice sheet fluctuations 10,000–70,000 yr ago as inferred from deposits on the Reykjanes Ridge, southeast of Greenland, *Quat. Res.*, *49*, 171–182.

Lambeck, K., and J. Chappell (2001), Sea level change through the last glacial cycle, *Science*, *292*, 679–686.

LaRocque, A., J.-M. M. Dubois, and B. Leblon (2003), Characteristics of late-glacial ice-dammed lakes reconstructed in the Appalachians of southern Quebec, *Quat. Int.*, *99–100*, 73–88.

Lekens, W. A. H., H. P. Sejrup, H. Haflidason, G. Ø. Petersen, B. Hjelstuen, and G. Knorr (2005), Laminated sediments preceding Heinrich event 1 in the northern North Sea and southern Norwegian Sea: Origin, processes and regional linkage, *Mar. Geol.*, *216*, 27–50.

Mangerud, J., V. Astakhov, M. Jakobsson, and J. I. Svendsen (2001), Huge ice-age lakes in Russia, *J. Quat. Sci.*, *16*, 773–777.

Mangerud, J., R. Lovlie, S. Gulliksen, A. K. Hufthammer, E. Larsen, and V. Valen (2003), Paleomagnetic correlations between Scandinavian ice-sheet fluctuations and Greenland Dansgaard-Oeschger events, 45,000–25,000 yr B. P., *Quat. Res.*, *59*, 213–222.

Mangerud, J., M. Jakobsson, H. Alexanderson, V. Astakhov, G. K. C. Clarke, M. Henriksen, C. Hjort, G. Krinner, J.-P. Lunkka, and P. Moller (2004), Ice-dammed lakes and rerouting of the drainage of northern Eurasia during the last glaciation, *Quat. Sci. Rev.*, *23*, 1313–1332.

Martrat, B., J. O. Grimalt, J. Villanueva, S. van Kreveld, and M. Sarnthein (2003), Climatic dependence of the organic matter contributions in the north eastern Norwegian Sea over the last 15,000 years, *Org. Geochem.*, *34*, 1057–1070.

McManus, J. F., D. W. Oppo, and J. L. Cullen (1999), A 0.5-million-year record of millennial-scale climate variability in the North Atlantic, *Science*, *283*, 971–975.

Miller, M. C., I. N. McCave, and P. D. Komar (1977), Threshold of sediment motion under unidirectional currents, *Sedimentology*, *24*, 507–527.

Mook, W. G., J. C. Bommerson, and W. H. Stavermen (1974), Carbon isotope fractionation between dissolved bicarbonate and gaseous carbon dioxide, *Earth Planet. Sci. Lett.*, *22*, 169–176.

Moros, M., A. Kuijpers, I. Snowball, S. Lassen, D. Backstrom, F. Gingele, and J. McManus (2002), Were glacial iceberg surges in the North Atlantic triggered by climatic warming?, *Mar. Geol.*, *192*, 393–417.

Nam, S. I. (1997), Late Quaternary glacial history and paleoceanographic reconstructions along the East Greenland continental margin: Evidence from high-resolution records of stable isotopes and ice-rafted debris, *Ber. Polarforsch.*, *241*, 138.

Olsen, S. M., G. Shaffer, and C. J. Bjerrum (2005), Ocean oxygen isotope constraints on mechanisms for millennial-scale climate variability, *Paleoceanography*, *20*, PA1014, doi:10.1029/2004PA001063.

Oppo, D. W., J. F. McManus, and J. L. Cullen (1998), Abrupt climate events 500,000 to 340,000 years ago: Evidence from subpolar North Atlantic sediments, *Science*, *279*, 1335–1338.

Orvik, K. A., and P. Niiler (2002), Major pathways of Atlantic water in the northern North Atlantic and Nordic Seas toward Arctic, *Geophys. Res. Lett.*, *29*(19), 1896, doi:10.1029/2002GL015002.

Pirrung, M., D. Fütterer, H. Grobe, J. Matthiessen, and F. Niessen (2002), Magnetic susceptibility and ice-rafted debris in surface sediments of the Nordic Seas: Implications for isotope stage 3 oscillations, *Geo Mar. Lett.*, *22*, 1–11.

Rahmstorf, S. (2003), Timing of abrupt climate change: A precise clock, *Geophys. Res. Lett.*, *30*(10), 1510, doi:10.1029/2003GL017115.

Ramm, M. (1988), A stratigraphic study of late Quaternary sediments on the Vøring Plateau, eastern Norwegian Sea, *Mar. Geol.*, *83*, 159–191.

Rasmussen, T. L., and E. Thomsen (2004), The role of the North Atlantic Drift in the millennial timescale glacial climate fluctuations, *Palaeogeogr. Palaeoclimatol. Palaeoecol.*, *210*, 101–116.

Rasmussen, T. L., E. Thomsen, W. T. C. E. van Weering, and L. Labeyrie (1996), Rapid changes in surface and deep water conditions at the Faeroe margin during the last 58,000 years, *Paleoceanography*, *11*, 757–771.

Rasmussen, T. L., T. C. E. v. Weering, and L. Labeyrie (1997), Climatic instability, ice sheets and ocean dynamics at high northern latitudes during the last glacial period (58–10 ka), *Quat. Sci. Rev.*, *15*, 1–10.

Rasmussen, T. L., D. Backstrom, J. Heinemeier, K. D. Klitgaard, P. C. Knutz, A. Kuijpers, S. Lassen, E. Thomsen, S. R. Troelstra, and T. C. E. van Weering (2002), The Faroe-Shetland gateway: Late Quaternary water mass exchange between the Nordic seas and the northeastern Atlantic, *Mar. Geol.*, *188*, 165–192.

Rasmussen, T. L., E. Thomsen, S. R. Troelstra, A. Kuijpers, and M. A. Prins (2003), Millen-

nial-scale glacial variability versus Holocene stability: Changes in planktic and benthic foraminifera faunas and ocean circulation in the North Atlantic during the last 60,000 years, *Mar. Micropaleontol.*, *47*, 143–176.

Raunholm, S., H. P. Sejrup, and E. Larsen (2003), Late glacial landform associations at Jaeren (SW Norway) and their glaci-dynamic implications, *Boreas*, *32*, 462–475.

Reimer, P. J., and R. W. Reimer (2001), A marine reservoir correction database and on-line interface, *Radiocarbon*, *43*, 461–463.

Richter, T. O., S. Lassen, T. C. E. v. Weering, and H. d. Haas (2001), Magnetic susceptibility pattern sand provenance of ice-rafted material at Feni Drift, Rockall Trough: Implications for the history of the British-Irish ice sheet, *Mar. Geol.*, *173*, 37–54.

Roche, D., D. Paillard, and E. Cortijo (2004), Constraints on the duration and freshwater release of Heinrich event 4 through isotope modelling, *Nature*, *432*, 379–382.

Rohling, E. J., R. Marsh, N. C. Wells, M. Siddall, and N. R. Edwards (2004), Similar meltwater contributions to glacial sea level changes from Antarctic and northern ice sheets, *Nature*, *430*, 1016.

Sachs, J. P., and S. J. Lehman (1999), Subtropical North Atlantic temperatures 60,000 to 30,000 years ago, *Science*, *286*, 756–759.

Sarnthein, M., et al. (1995), Variations in Atlantic surface ocean paleoceanography, 50°–80°N: A time-slice record of the last 30,000 years, *Paleoceanography*, *10*, 1063–1094.

Sarnthein, M., et al. (2001), Fundamental modes and abrupt changes in Northern Atlantic circulation and climate over the last 60 ky: Concepts, reconstruction and numerical modeling, in *The Northern North Atlantic: A Changing Environment*, edited by P. Schäfer et al., pp. 365–410, Springer, New York.

Scambos, T. A., C. Hulbe, M. Fahnestock, and J. Bohlander (2000), The link between climate warming and break-up of ice shelves in the Antarctic Peninsula, *J. Glaciol.*, *46*, 516–530.

Schulz, M. (2002), On the 1470-year pacing of Dansgaard-Oeschger warm events, *Paleoceanography*, *17*(2), 1014, doi:10.1029/2000PA000571.

Schulz, M., W. H. Berger, M. Sarnthein, and P. M. Grootes (1999), Amplitude variations of 1470-year climate oscillations during the last 10,000 years linked to fluctuations of continental ice mass, *Geophys. Res. Lett.*, *26*, 3385–3388.

Schulz, M., A. Paul, and A. Timmermann (2004), Glacial-interglacial contrast in climate variability at centennial-to-millennial timescales: Observations and conceptual model, *Quat. Sci. Rev.*, *23*, 2219–2230.

Shaffer, G., S. M. Olsen, and C. J. Bjerrum (2004), Ocean subsurface warming as a mechanism for coupling Dansgaard-Oeschger climate cycles and ice-rafting events, *Geophys. Res. Lett.*, *31*, L24202, doi:10.1029/2004GL020968.

Siddall, M., E. J. Rohling, A. Almogi-Labin, C. Hemleben, D. Meischner, I. Schmelzer, and D. A. Smeed (2003), Sea-level fluctuations during the last glacial cycle, *Nature*, *423*, 853–858.

Smith, L. M., and J. T. Andrews (2000), Sediment characteristics in iceberg dominated fjords, Kangerlussuaq region, East Greenland, *Sediment. Geol.*, *130*, 11–25.

Spero, H. J., J. Bijma, D. W. Lea, and B. E. Bemis (1997), Effect of seawater carbonate concentration on foraminiferal carbon and oxygen isotopes, *Nature*, *390*, 497–500.

Spielhagen, R. F., and H. Erlenkeuser (1994), Stable oxygen and carbon isotopes in planktic foraminifers from Arctic Ocean surface sediments: Reflection of the low salinity surface water layer, *Mar. Geol.*, *119*, 227–250.

Spielhagen, R. F., K.-H. Baumann, H. Erlenkeuser, N. R. N. R. Nowaczyk, N. Norgaard-Pedersen, C. Vogt, and D. Weiel (2004), Arctic Ocean deep-sea record of northern Eurasian ice sheet history, *Quat. Sci. Rev.*, *23*, 1455–1483.

Stuiver, M., P. J. Reimer, and T. F. Braziunas (1998), High-precision radiocarbon age calibration for terrestrial and marine samples, *Radiocarbon*, *40*, 1127–1151.

Teller, J. T. (1995), History and drainage of large ice-dammed lakes along the Laurentide Ice Sheet, *Quat. Int.*, *28*, 83–92.

Valen, V., J. Mangerud, E. Larsen, and A. K. Hufthammer (1996), Sedimentology and stratigraphy in the cave Hamnsundhelleren, western Norway, *J. Quat. Sci.*, *11*, 185–201.

van Kreveld, S., M. Sarnthein, H. Erlenkeuser, P. Grootes, S. Jung, M. J. Nadeau, U. Pflaumann, and A. Voelker (2000), Potential links between surging ice sheets, circulation changes, and the Dansgaard-Oeschger cycles in the Irminger Sea, 60–18 kyr, *Paleoceanography*, *15*, 425–442.

Vidal, L., L. Labeyrie, E. Cortijo, M. Arnold, J. C. Duplessy, E. Michel, S. Becque, and T. C. E. van Weering (1997), Evidence for changes in the North Atlantic Deep Water linked to meltwater surges during the Heinrich events, *Earth Planet. Sci. Lett.*, *146*, 13–27.

Villanueva, J., J. O. Grimalt, E. Cortijo, L. Vidal, and L. Labeyriez (1997), A biomarker approach to the organic matter deposited in the North Atlantic during the last climatic cycle, *Geochim. Cosmochim. Acta*, *61*, 4633–4646.

Voelker, A. H. L. (2002), Global distribution of centennial-scale records for marine isotope stage (MIS) 3: A database, *Quat. Sci. Rev.*, *21*, 1185–1214.

Voelker, A., M. Sarnthein, P. Grootes, H. Erlenkeuser, C. Laj, C. Mazaud, M.-J. Nadeau, and M. Schleicher (1998), Correlation of marine ^{14}C ages from the Nordic Seas with the GISP2 isotope record: Implications for ^{14}C calibration beyond 25 ka BP, *Radiocarbon*, *40*, 517–534.

Voelker, A. H. L., P. M. Grootes, M.-J. Nadeau, and M. Sarnthein (2000), Radiocarbon levels in the Iceland Sea From 25–53 kyr and their link to the Earth's magnetic field intensity, *Radiocarbon*, *42*, 437–452.

Volkmann, R., and M. Mensch (2001), Stable isotope composition $\delta^{18}O$, $\delta^{13}C$ of living planktic foraminifers in the outer Laptev Sea and the Fram Strait, *Mar. Micropaleontol.*, *42*, 163–188.

Vorren, T. O., and J. S. Laberg (1997), Trough mouth fans—Palaeoclimate and ice-sheet monitors, *Quat. Sci. Rev.*, *16*, 865–881.

Waelbroeck, C., J.-C. Duplessy, E. Michel, L. Labeyrie, D. Pailard, and J. Duprat (2001), The timing of the deglaciation in North Atlantic climate records, *Nature*, *412*, 470.

Weinelt, M., E. Vogelsang, M. Kucera, U. Pflaumann, M. Sarnthein, A. Voelker, H. Erlenkeuser, and B. A. Malmgren (2003), Variability of North Atlantic heat transfer during MIS 2, *Paleoceanography*, *18*(3), 1071, doi:10.1029/2002PA000772.

Wilson, L. J., and W. E. N. Austin (2002), Millennial and sub-millennial-scale variability in sediment colour from the Barra Fan, NW Scotland: Implications for British ice sheet dynamics, in *Glacier-Influenced Sedimentation on High-Latitude Continental Margins*, edited by J. A. Dowdeswell and C. Ó. Cofaigh, pp. 349–365, Geol. Soc. of London, London.

Zhang, J., P. D. Quay, and D. O. Wilbur (1995), Carbon isotope fractionation during gas-water exchange and dissolution of CO_2, *Geochim. Cosmochim. Acta*, *59*, 107–114.

H. Haflidason, W. A. H. Lekens, and H. P. Sejrup, Department of Earth Science, University of Bergen, Allegaten 41, N-5007 Bergen, Norway. (wim.lekens@geo.uib.no)

J. Knies, Geological Survey of Norway, Leiv Eirikssons v 39, N-7491 Trondheim, Norway.

T. Richter, Royal Netherlands Institute for Sea Research, Landsdiep 4, 1797 SZ Den Hoorn (Texel), Netherlands.